

Prototyping a Virtual Colonoscopy System

A master's thesis presented

by

Dirk Matthias Bartz

Computer Graphics Group

Department of Computer Science

University of Erlangen-Nürnberg, Germany

December, 1996

Copyright by

Dirk Bartz

1996

Ein Prototyp für eine virtuelle Dickdarmendoskopie

Diplomarbeit im Fach Informatik

vorgelegt von

Dirk Matthias Bartz

geb. am 22.07.1967 in Simmern/Hunsrück

Betreuende Hochschullehrer:

Prof. Dr. Arie Kaufman (StonyBrook)

Prof. Dr. Thomas Ertl (IMMD9)

Beginn der Arbeit: 01.07.1996

Abgabe der Arbeit: 31.12.1996

Ich versichere, daß ich die Arbeit ohne fremde Hilfe und ohne Benutzung anderer als der angegebenen Quellen angefertigt habe und daß die Arbeit in gleicher oder ähnlicher Form noch keiner anderen Prüfungsbehörde vorgelegen hat und von dieser als Teil einer Prüfungsleistung angenommen wurde. Alle Ausführungen, die wörtlich oder sinngemäß übernommen wurden, sind als solche gekennzeichnet.

Erlangen, den 21.12.1996 _____

Überblick

Enddarmkrebs (Krebs des Dickdarms oder des Rectums) ist die zweitgrößte Ursache für den Tod durch Krebs in den USA. Jährlich werden allein in den USA etwa 158.000 Diagnosen gestellt. Die Wahrscheinlichkeit für die Erkrankung an Enddarmkrebs liegt für die Amerikaner bei 1:20, die Sterblichkeit bei 2.5% [CBW95]. Seine frühe Entdeckung und Behandlung ist von hoher Bedeutung für das Überleben der Patienten. Leider entwickeln sich die Symptome erst in einer späten Phase der Krankheit. Aus diesem Grund scheint eine Reihenuntersuchung von Patienten einer bestimmten Risikogruppe, z.B. ab einem bestimmten Alter, angebracht. Gegenstand der Untersuchung ist die Suche im Dickdarm nach Polypen mit einem Durchmesser von mehr als 5 mm. Diese Polypen haben eine hohe Wahrscheinlichkeit, bösartig zu sein.

Medizinische Grundlagen

Zur Zeit existieren fünf verschiedene Untersuchungsmethoden zur Diagnose von Enddarmkrebs, von denen allerdings nur zwei zur Untersuchung des kompletten Dickdarms geeignet sind:

1. Barium Enema

Zu Beginn dieser Methode wird Barium in den Dickdarm eingeführt und auf einem Röntgenschirm bei niedriger Bestrahlung überwacht. Anschließend werden Übersichtsaufnahmen aus verschiedenen Blickwinkeln erzeugt. Polypen können durch Formdefekte (z.B. Ausstülpungen) der Bariumkolorierung erkannt werden. Diese Prozedur ist nicht invasiv und relativ günstig (\$400 [HLVK96]). Leider erfordert sie aber einen hohen Grad an Kooperation seitens des Patienten. Die Sensitivität liegt in dem Bereich von 78% bis zu 80-95% bei Polypen größer als 1 cm und ist damit nur eingeschränkt brauchbar [CBW95]. Ein weiterer Nachteil ist die relativ hohe Röntgenbestrahlung des Abdomen und damit des reproduktiven Systems des Patienten.

2. Optische Dickdarmendoskopie

Die optische Dickdarmendoskopie wird in medizinischen Veröffentlichung als geeignetes Verfahren zur Reihenuntersuchung von Dickdärme empfohlen [CBW95]. Hierbei wird eine optische Sonde in den Dickdarm des Patienten eingeführt, der intravenös sediert und dessen Dickdarm mit Luft aufgefüllt werden muß.

Verbunden mit der Dickdarmendoskopie ist ein geringes Risiko der Perforation. Abhängig von technischen Problemen und der Belastung des Patienten kann in einigen Fällen der Dickdarm - insbesondere der vordere Bereich - nicht komplett untersucht werden. Wirtschaftlich gesehen ist diese Methode teurer als die vorhergehende: Ein trainierter Arzt braucht ungefähr 40 bis 50 Minuten, um diese Untersuchung durchzuführen. Die Kosten bewegen sich dabei im Bereich von \$1.300 bis \$1.900. Die Sensitivität liegt bei über 90%, auch bei Polypen kleiner als 1 cm [CBW95].

In dieser Arbeit

In dieser Arbeit wird eine alternative Methode zur Untersuchung des ganzen Dickdarms vorgeschlagen, die virtuelle Dickdarmendoskopie. Dieses Verfahren besteht im wesentlichen aus drei Bearbeitungsschritten:

1. Klinischer Abschnitt

Nach einer Aufblähung des Dickdarms des Patienten mit Hilfe von Luft wird ein Volumendatensatz des Abdomen mittels mehrerer CT-Projektionen erzeugt. Die Aufblähung des Dickdarms ist notwendig um ihn vollständig zu entfalten und um einen guten Kontrast für das Segmentierungsverfahren im nächsten Schritt zu erreichen.

2. Vorbearbeitung durch eine Workstation

Im ersten Vorbearbeitungsschritt wird die Segmentierung des Dickdarms aus dem Volumendatensatz mit einem einfachen binären Segmentierungsverfahren vorgenommen. Anhand der segmentierten Dickdarmvoxel wird ein Skelett des Dickdarms erzeugt.

Im nächsten Vorbearbeitungsschritt wird entlang des Dickdarmskeletts eine Unterteilung der Dickdarmvoxel in Segmente vorgenommen und anschließend eine Isofläche mittels des MarchingCube-Algorithmus extrahiert.

Schließlich werden anhand der Dickdarmvoxelunterteilung zwei Potentialfelder berechnet, die zur Navigation verwendet werden.

3. Interaktive navigationsunterstützte Untersuchung des Dickdarms

Ein Visibilitätsalgorithmus, basierend auf der Dickdarmunterteilung, wird angewendet und ein interaktiver Fly-Through durch diesen Dickdarm erzeugt. Mit Hilfe eines halbautomatischen Kameramodells wird die Orientierung innerhalb dieses Organs und die Interaktivität während der Untersuchung gewährleistet.

Erste Erfahrungen

Der Umgang mit einem Endoskop und die Orientierung durch das optische System des Endoskops sind sehr schwierig, so daß Ärzte ein mehrjähriges Training absolvieren, um ein solches Instrument sicher bedienen zu können. Dieses Training fehlt den klinischen Projektpartnern der Radiologie des University Hospitals at Stony Brook, so daß ein echter Vergleich durch eine klinischen Evaluation - die in Kürze vorgenommen wird - geleistet werden kann. Erste Erfahrungen liegen jedoch durch die Zusammenarbeit mit den klinischen Projektpartner vor. Hierbei wurden die Ergebnisse einer optischen Dickdarmendoskopie mit denen der virtuellen Dickdarmendoskopie bei einem Patienten gegenüber gestellt.

Es zeigte sich, daß das System der virtuellen Dickdarmendoskopie sehr intuitiv bedienbar und in weniger als einer halben Stunde beherrscht werden konnte. Formdefekte konnten an vergleichbaren Positionen wie in der optischen Dickdarmendoskopie nachgewiesen werden. Leider war eine endgültige Aussage nicht möglich, da durch ungenaue Positionsangaben des optischen Verfahrens und durch Segmentierungsprobleme des virtuellen Verfahrens einige Fragestellungen nicht entscheidbar waren.

Besonders problematisch ist das Segmentierungsproblem. Das aktuelle binäre Segmentierungsverfahren reicht nur bei einem vollständig von Stuhl gesäuberten Dickdarm aus. Diese Annahme ist jedoch nicht realistisch, was dazu führte daß Stuhl nicht von der eigentlichen Oberfläche unterschieden werden kann. Leider sind nicht entfernter Stuhl und Polypen in der Form sehr ähnlich, so daß eine endgültige Aussage nicht möglich ist. Eine mögliche Lösung für dieses Problem scheint die Änderung des Dichtewertes des Stuhls - mit Hilfe eines speziellen Kontrastmittelcocktails - zu sein. Die zugehörige Untersuchung dieser Problemlösung wird in nächster Zeit vorgenommen.

Zusammenfassung

Die Vorteile der vorgestellten Methode liegen in der hohen Flexibilität der Navigation und in der Einfachheit der Bedienung. Der medizinische Abschnitt der Untersuchung beschränkt sich auf das CT des Abdomen des Patienten und der Einführung von Luft zur Verbesserung des Kontrastes. Insgesamt dauert dies ca. zehn Minuten und verursacht Kosten von ungefähr \$400.

Nachteilig wirken sich die Beschränkungen durch die CT-Aufnahmen aus, so kann z.B. Stuhl nicht eindeutig von Polypen unterschieden werden. Außerdem ist eine Biopsie - eine durch eine kleine Zange bei der optischen Dickdarmendoskopie entnommene Gewebeprobe - nicht möglich. Auch die Genauigkeit der sogenannte "virtuelle Biopsie" durch eine Area-of-

Interest-Selektion ist durch die Auflösung des Computertomographen beschränkt und reicht nicht an die Auflösung moderner Mikroskope bei der physischen Biopsie heran.

Insgesamt zeichnet sich die virtuelle Dickdarmendoskopie durch eine einfachere Bedienung und hohe Bildqualität aus. Insbesondere scheint die unmittelbare Aussagekraft im Vergleich zur Barium Enema deutlich erhöht zu sein.

Abstract

Screening of the colon of patients of an advanced age can lead to an early detection of colorectal cancer. The current available methods to explore the whole colon are rather difficult in handling and interpretation, but also of great discomfort to the patient.

In this thesis, we present an alternative method, called Virtual Colonoscopy. After a CT scan of the abdomen of the patient is performed, a segmentation of the colon from this dataset is generated. A visibility algorithm, based on a subdivision of the segmented colon, is applied to compute an interactive fly-through this colon. A camera model, utilizing the guided-navigation paradigm, guarantees the orientation and the interactivity of the actions of the examiner.

Acknowledgments

First of all, I would like to thank my advisors Arie Kaufman and Thomas Ertl, who gave me the opportunity to do my master project in the Visualization Lab of the State University of New York at Stony Brook. It really was a great experience.

I would also like to thank Lichan Hong and Shigeru Muraki, my collaborators of the Colonoscopy project. It was a pleasure working with them and discussing the problems of our project. In addition, I like to thank Ajaj Viswambharan and Mark Wax of the Radiology department of the University Hospital at Stony Brook.

Furthermore, I would like to thank the members of the Visualization Lab: Ingmar Bitter, Baoquan Chen, Rui Chiou, Francine Evans, Akio Doi, Ell-Sana Jihad, Hanspeter Pfister, Claudio Silva, Ikuko Takanashi and Amitabh Varshney. Especially I would like to thank Pat Tonra, who answered uncountable cries for help.

Last but not least, I would like to express my deep gratitude to my sponsor and mother Elisabeth Bartz. Without her support, my stay at Stony Brook would not have been possible.

Table of Content

1. Introduction	1
2. Medical Foundations	3
2.1 Anatomy of the Colon	3
2.2 Medical procedures	5
3. Concepts and Algorithms.....	7
3.1 System Architecture.....	7
3.2 Subdivision, Visibility and Rendering.....	9
3.2.1 Overview.....	9
3.2.2 The Subdivision Scheme.....	9
3.2.3 The Visibility and Rendering Algorithm.....	18
3.2.4 Results	22
3.3 The Navigation Model.....	23
3.4 The User-Interface	25
4. Two Methods for a Colonoscopy.....	29
4.1 A Optical Colonoscopy	29
4.2 A Virtual Colonoscopy	31
4.3 Discussion	34
5. Conclusion and Future Work.....	35
5.1 Conclusion	35
5.2 Future work	36

Appendices

A Class Structure of VICON/i	39
B File Structure of the Virtual Colonoscopy System	40
C References	43

1. Introduction

Computer Graphic methods have been used for many years in medical applications. Since the invention of image producing techniques like Computer Tomography (CT) in the early seventies, the popularity of these methods has been on the rise.

In the early days of Computer Graphics, the methods were limited to 2D image processing techniques to generate and display the slice projections of CT data. Soon, methods of Computer Aided Geometric Design (CAGD) had been introduced; i.e. Vannier et al. used Bezier curves to support the planning of cranial surgery [VMW83].

Rapid improvements of the processing power of computers and the development of specialized graphics hardware have led to a steadily increasing quality. In the late eighties, the simulation of the behavior of human tissue became a growing research field in visualization. Pieper used Finite Element Method (FEM) to simulate cuts through the tissue of the human skin to predict the outcome of plastic surgery [Piep92]. In [Wate87] Waters presented a model for artificial muscle actors and extended it with Terzopoulos to a facial tissue model [WT90].

Bartz used a simplified implementation of this tissue model and Triangular B-Splines [DMS92] to generate possible visible results of craniofacial corrective surgery [Bart95]. Keeve et.al. used a polygonal-based extension of this model, combined with FEM to improve the quality of the simulation [KGPG96]. Koch et. al. proposed a similar method for their virtual medicine system [KGCB96].

With the development of Direct Volume Rendering (DVR) volumetric information could be incorporated into these techniques to increase the accuracy of the results. An early overview of the techniques in use in medical applications can be found in [FLP89]. Höhne et al. presented VOXEL-MAN, in which segmented CT/MRI data were combined with an expert system to provide an anatomical atlas [HPRS94].

In 1995 Hong et. al. presented an automatic fly-through colonoscopy - using a planned-navigation paradigm - of the Visible Male [HKWV95]. In this system DVR techniques were used to generate frames of the automatic fly-through. Due to high computational costs it was not possible to use these techniques for an interactive approach. Lorensen et al. proposed an automatic fly-through endoscopy based on surface rendering and a robot path planning algorithm. The major drawback of this approach is the calculation of the camera position - in most cases this position is too close to the colon wall, which limits the view.

In this thesis we present a prototype for a virtual endoscopy of the human colon (colonoscopy). Our system is based on the system presented in [HMHK96], with a suitable user-interface, an improved rendering algorithm, and camera model proposed in [HR85]. In contrast to previous work, our approach is using an interactive, center-path camera model utilizing the guided-navigation paradigm.

The thesis is organized as follows: In chapter two we discuss the medical issues of this project; this contains the anatomy of the human colon and a brief description of two medical procedures for the examination of the colon. Chapter three describes the techniques used in our system - the new subdivision scheme for the visibility algorithm and some user-interface issues. Chapter four presents our virtual colonoscopy and a comparison with the optical colonoscopy. Ultimately, in chapter five, we state our conclusion and discuss future work in this field.

2. Medical Foundations

The second leading cause of cancer death in the USA is cancer of the colon or the rectum. Every year approximately 158,000 diagnoses of these kinds of cancers are cited. The annual incidence of colorectal cancer is the second largest in women - after breast cancer - and the third largest in men - after lung or prostate cancer. The probability for Americans at the age of 50 of developing colorectal cancer is 1:20, the likelihood of dying from this cancer, is 2.5%.

In many cases, colorectal cancer is discovered after the development of symptoms at a late stage of the disease. However, early detection and early treatment are crucial for the survival of patients.

So far, five methods can be used for diagnostic purposes:

- Digital Rectal Examination
- Fecal Occult Blood Tests
- Flexible Sigmoidoscopy
- Barium Enema
- Optical Colonoscopy

These methods vary greatly in terms of safety, ease of performance and accuracy, but only the latter two methods can be used to examine the **whole** colon. (A brief description of these methods can be found in the second section of this chapter.) The following section gives a brief overview of the anatomy of the human colon.

2.1 Anatomy of the Colon

The colon is part of the *large intestine*, and begins with the *appendix* and ends with *the rectum* and the *anal canal*. In total, the *large intestine* is approximately 1.5 m long, the colon being its largest part.

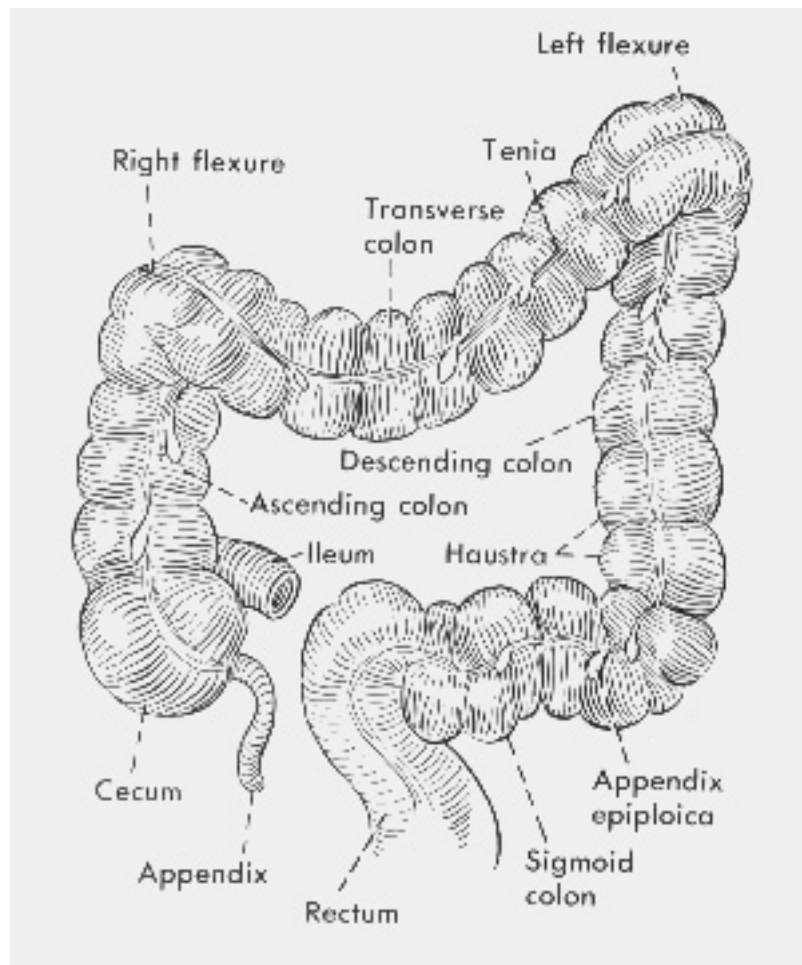


Fig. 2.1: From [HR85]: The large intestine

The colon consists of three parts. The *ascending colon* roughly starts after the *appendix* and *cecum* and continues up to the *right (colic) flexure* (Fig. 2.1). After the *right flexure*, the colon continues with the *transverse colon*. It travels across the abdomen to the *left (colic) flexure*. Fig. 2.2 shows that the *transverse colon* does not necessarily run straight. In many cases it runs twistedly from right to left. The *descending colon* begins after the *left flexure* and leads to the *sigmoid colon*, and ultimately to the *rectum*.

The *ascending* and *descending colons* are fixed to the *pelvic wall*. In contrast, the *transverse colon* has more freedom to move; it is only suspended on a *peritoneal fold*.

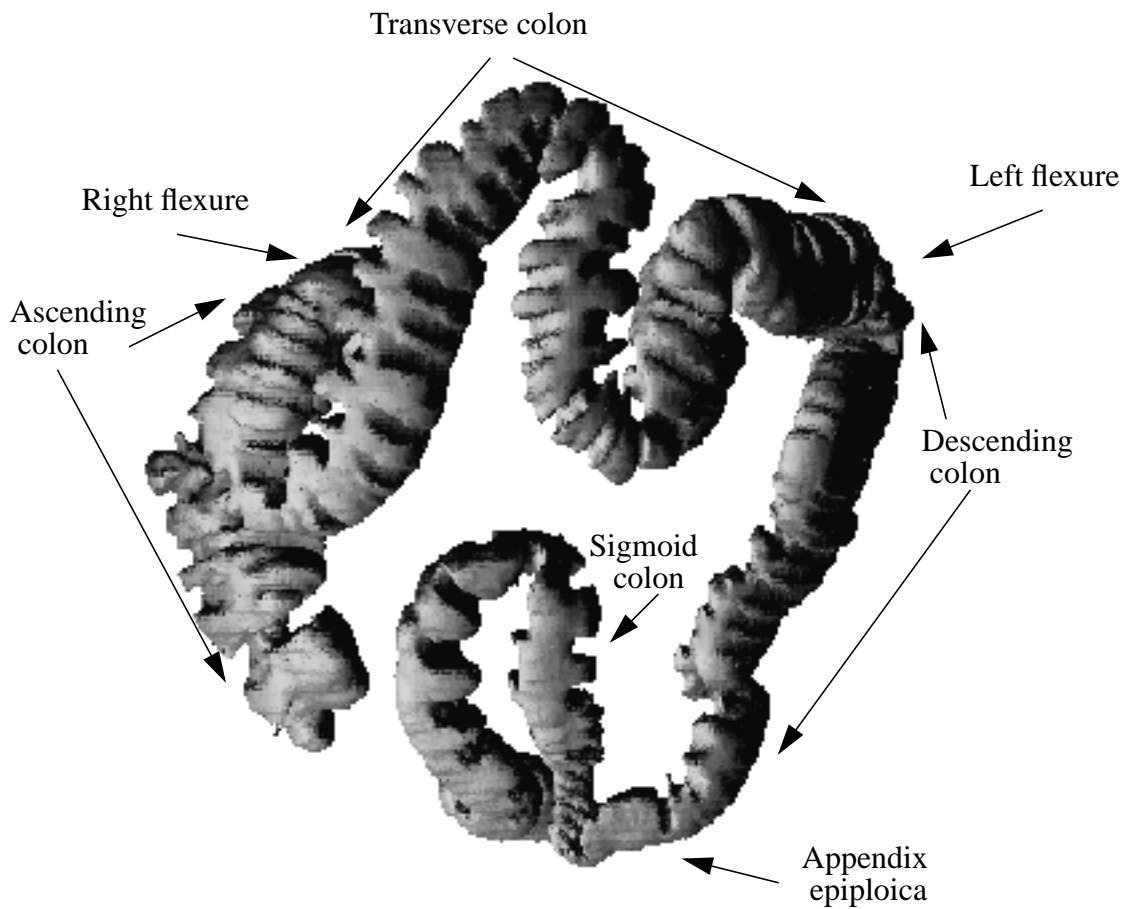


Fig. 2.2: A patient's colon - coronal view

2.2 Medical procedures

In this section, we describe two procedures for the examination of the human colon. The goal of both procedures is to find polyps. Polyps of a size greater than 5 mm have a high probability of being malignant.

1. Barium Enema

At the beginning of the procedure, barium is introduced into the colon and monitored with low-intensity x-rays. Thereafter, *overhead* x-rays are taken from different viewing angles. Polyps are detected by shape defects of the barium coloring inside the colon.

This procedure is non-invasive and relatively cheap (\$400 [HLVK96]). However, it requires cooperation from the patient and an experienced interpreter. According to the literature, the sensitivity ranges from 78% [HLVK96] to 80-95% for polyps larger than 1 cm [CBW95]. Additionally, a high dose of radioactivity is introduced to an area close to the reproductive system.

2. Optical Colonoscopy

The usage of endoscopes as a screening tool for colorectal cancer has been recommended in medical publications [CBW95]. This method utilizes a fiber optical probe to examine the colon. For this invasive procedure, the patient must be intravenously sedated and the colon inflated with air. Associated with the optical colonoscopy is a small risk of perforations of the colon. Additionally, depending on technical difficulties or patient discomfort, the colon can not be fully examined, especially the proximal colon. Economically, the optical colonoscopy is more expensive than the Barium Enema; a trained physician takes about 40 to 50 minutes to perform this procedure. Costs range between \$1,300 and \$1,900. The sensitivity of the optical colonoscopy is above 90%. Section 4.1 presents some visual results of an optical colonoscopy.

3. Concepts and Algorithms

In this chapter, after a short overview of the system architecture, we describe the main design issues of the Virtual COloNoscopy (VICON): the subdivision scheme, the visibility and rendering algorithm, the navigation model and some user-interface issues. The navigation model was not the focus of this thesis. Therefore, it is only described very briefly. Further discussion can be found in [HMBK97].

3.1 System Architecture

The VICON system consists of two computer-based stages: the pre-processing stage and the interactive rendering stage.

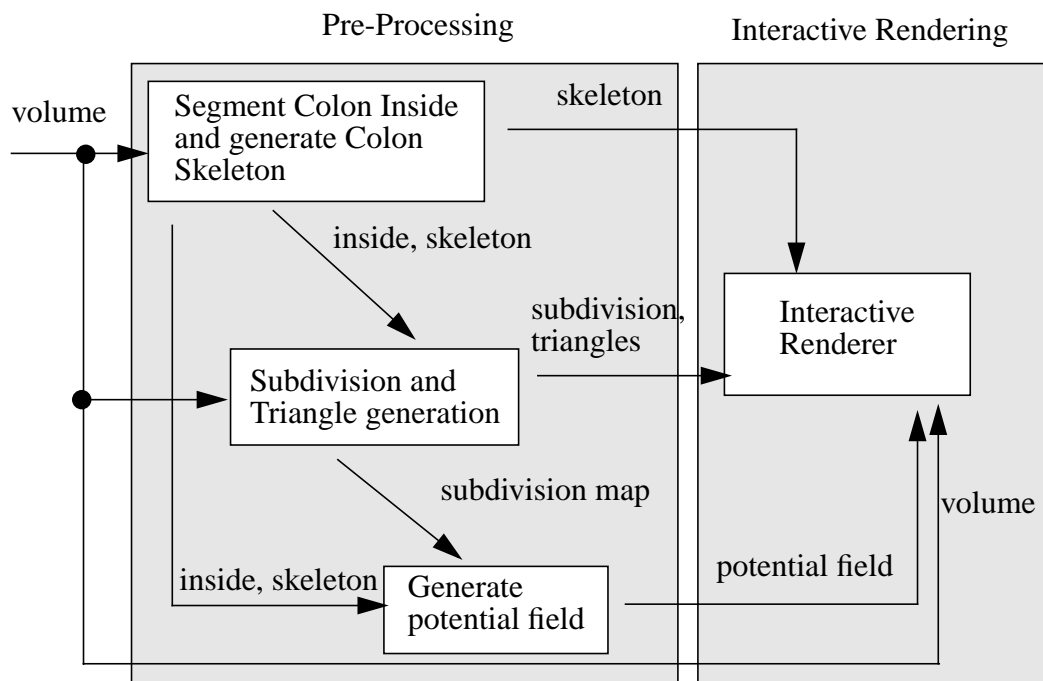


Fig. 3.1: System architecture

There are three pre-processing steps. In the first step, VICON/seg, all the voxels associated with the inside of the colon - the inside voxels - are segmented. Due to the inflated air, we have good contrast between the inside and the outside of the colon. Therefore, it is possible to apply a simple binary segmentation with a certain isovalue. Additionally, the skeleton of the colon is generated. The skeleton is a 26-connected line from an inside voxel near the Appendix to an inside voxel near the Rectum. Further description can be found in [HKWV95].

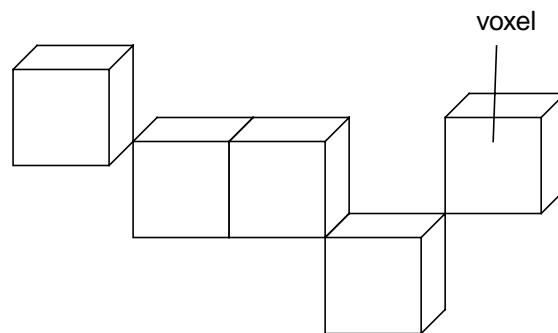


Fig. 3.2: A 26-connected voxel line segment

In the second step, VICON/sub, the subdivision of the inside voxels along the skeleton is generated, which divides the inside voxels into *segments* (see section 3.2.2). Thereafter, the surfaces of the colon *segments* - the *cells* - are extracted.

Definiton 3.1: A *segment* is a subset of inside voxels of the colon. All *segments* are disjoint and the union of all *segments* is equal to the inside voxels of the colon.

Definiton 3.2: A *cell* is the extracted and triangulated surface of a *segment*.

In the third and last pre-processing step, VICON/p the potential field for the navigation model is generated (see section 3.3). The results of all three pre-processing steps are used in the second stage, the interactive rendering, VICON/i.

3.2 Subdivision, Visibility and Rendering

3.2.1 Overview

During one of the pre-processing steps, we generate a surface of the inside of the human colon using the Marching Cube algorithm [LC87]. Usually, the number of generated triangles is very high. Depending on the number of voxels of the colon surface, the triangles can number between a few hundred thousand and more than one million. See *Tab. 1* for an overview of some dataset sizes.

<i>Dataset</i>	<i>Dimension</i>	<i>#Triangles</i>	<i>#Cells</i>
Colon of Visible Male	582 x 405 x 254	130,429	40
patient data 3	512 x 512 x 406	774,956	99
patient data 4a	512 x 512 x 181	839,774	89
patient data 4b	512 x 512 x 361	1,277,891	137
patient data 9	512 x 512 x 367	606,249	50

Table 1: Dataset sizes

Most workstations, even SGI's high-performance graphic workstations with MaxImpact or InfiniteReality graphic hardware, are not able to render these amounts of triangles fast enough to obtain an interactive speed of 10 to 20 frames per second. In order to guarantee an interactive frame rate, we subdivide the whole colon surface into a set of *segments*. Each *segment* (actually, each *cell*) is rendered individually, and our visibility algorithm is applied.

3.2.2 The Subdivision Scheme

As mentioned before, the goal of the subdivision is the division of the colon surface by *subdivision planes* into a set of *segments*. Ideally, each segment has approximately the same size, to

guarantee a balanced frame rate. However, in some cases it is not possible, because of the twisted nature of the colon.

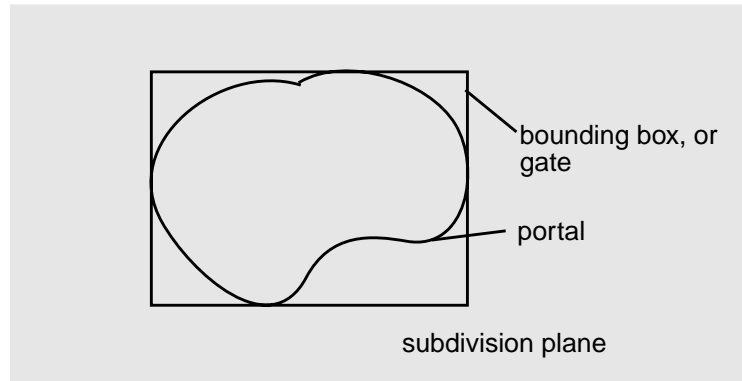


Fig. 3.3: Planes, Gates and Portals of the subdivision

In our terminology, we call the intersection of the *subdivision plane* with the inside voxels of the colon a *portal*, a term which is widely used in Virtual Reality to specify the connection between different *cells*.

Definiton 3.3: A *portal* is the intersection of the *subdivision plane* with the inside voxels of the colon. *Portals* separate *segments* from each other.

For the visibility algorithm, we use its bounding box as an approximation and call it a *gate* (see Fig. 3.3).

Definiton 3.4: A *gate* is the bounding box of a *portal*.

The major design issue is to determine which criteria to choose to find an appropriate subdivision. We divide our set of criteria into two groups: Mandatory and quality.

Mandatory criteria - these criteria must be met in order to generate a valid subdivision:

- The *portals* (not the *gates*) must not intersect each other. Otherwise, the distinction between the different *segments* would not be clear.
- Every voxel of the volume which is marked as inside the colon (inside voxel) must be part of exactly one *segment*. Otherwise, some voxels would not be rendered.

- The skeleton of the colon must not be disconnected. Otherwise, the subdivision along the skeleton cannot be finished.

Quality criteria must be met in order to generate a “good” subdivision:

- With respect to the processing time and the quality of the solution, we have to choose between a global or a local approach.
- The size of the *segments* should be feasible.
- The subdivision should be effective.

1. Global versus local approach

From the first pre-processing step, we have a 26-connect path through the whole colon; the skeleton. The examination of the colon is roughly performed along this skeleton. To compute the subdivision along the skeleton, two approaches are possible: a global or a local approach.

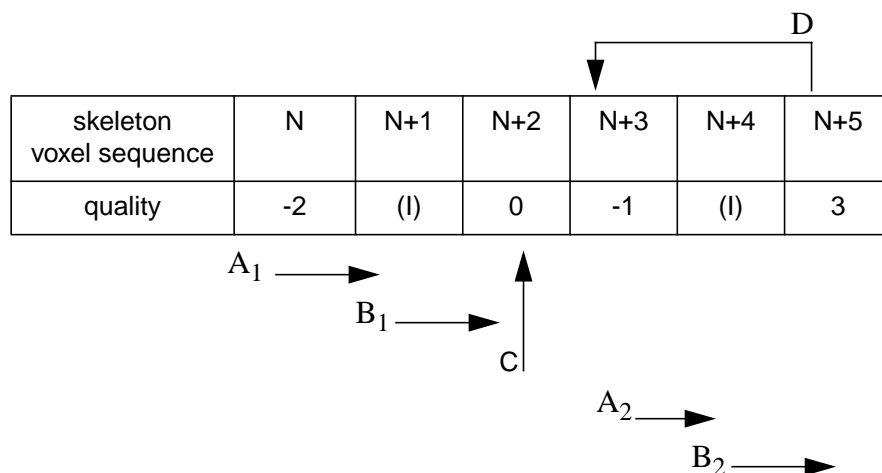


Fig. 3.4: In this example, we have a sequence of skeleton voxels. In the lower part of the box, the quality measure is specified: Zero is a “good” candidate, negative numbers are below a “good” evaluation, positive numbers are above a “good” evaluation. ‘(I)’ is invalid.

A: We move forward in our sequence, **B:** We skip an invalid candidate (according to mandatory criteria), **C:** We accept a “good” candidate, **D:** We go back to an older candidate

The complexity of a global approach computing an optimal solution is of a non-deterministic polynomial nature. For this reason, we choose the more practical local approach, which uses heuristics to compute a “good” solution.

Basically, we move along the skeleton path (see *Fig. 3.4*) and look for a possible *segment* boundary which suffices our quality criteria (A). During our walk along the path, we assume a certain linearity, so that the *segments* do not become smaller while moving towards the end of the path ($N+3$, $N+5$). However, local corrections are possible - if we pass a skeleton voxel which is worse than an earlier one (A_2 , B_2), we go back to the earlier candidate (D), which might be better than the current candidate.

2. Feasible *segment* sizes

One problem of the subdivision is deciding whether a *segment* has a feasible size. In this thesis, three methods are discussed: two heuristic methods and one analytic method.

Number of Surface Voxels

This heuristic depends on the number of surface voxel of a candidate for a *segment*. The basic assumption is that the number of triangles - which will be generated after the subdivision - is related to this number of surface voxels. It turns out that this method generates fairly good subdivisions. *Segments* with a larger number of surface voxels have a larger number of triangles, and vice versa.

Number of Inside Voxels

Similar to the previous method, this method depends on the number of inside voxels of a candidate. As presumed, the results are similar; a larger number of inside voxels is associated with a larger number of triangles actually generated.

<i>Method</i>	<i>#Segments / specified #segments</i>	<i>Average #triangles per cell</i>	<i>#Triangles per cell: max / min</i>	<i>Standard deviation</i>
Surface Voxels Dataset: Visible Male	40 ^a / 50	3,233	8,449 / 861	406.89

Table 2: Size distribution of subdivision schemes (The triangle-based method is not implemented.)

<i>Method</i>	<i>#Segments / specified #segments</i>	<i>Average #triangles per cell</i>	<i>#Triangles per cell: max / min</i>	<i>Standard deviation</i>
Inside Voxels Dataset: Visible Male	50 ^a / 50	2,669	8,449 / 830	387.29
Surface Voxels Dataset: Patient 4a	77 ^a / 100	10,747	471,48 / 826	181.62
Inside Voxels Dataset: Patient 4a	89 ^a / 100	9,401	47,148 / 1,836	312.24
Surface Voxels Dataset: Patient 9	37 ^a / 50	16,121	188,823 ^b / 935	2,320.08
Inside Voxels Dataset: Patient 9	45 ^a / 50	13,375	188,823 ^b / 935	2,512.64

**Table 2: Size distribution of subdivision schemes
(The triangle-based method is not implemented.)**

- a. For both methods, the same number of *segments* was specified.
- b. This large number of triangles is due to a part of the colon, where the skeleton path started later.

The second method produced a better controllable subdivision for all examined datasets - the number of *segments* is closer to the specified number of *segments* - than did the first one. Although, the statistical data suggested a better quality of the first method. A further examination was inconclusive; both methods generated a feasible subdivision.

Number of Triangles

This method is the only precise method, because the number of triangles can be directly balanced. Unfortunately, this method is computationally very expensive; for every *segment* candidate the triangles for the surface must be generated by a surface extraction algorithm, such as Marching Cube. This approach would greatly extend the execution time for a large dataset (patient 4a), which already takes about one hour. The expected improvement of the subdivision, using this method, does not justify the usage of this time-costly method.

3. Effective subdivision

Besides the control over the *segment* size of a subdivision, its effectiveness is very important. In this section, we examine three methods to generate an effective subdivision.

Skeleton Tangent

In this first implemented approach, the *portal* is generated with respect to the local tangent of the skeleton. After the calculation of the tangent in the neighborhood of a few adjunctive skeleton voxels, the component with the largest absolute value is chosen as the specification of the *portal*: i.e., if the x (or first) component is the largest, we choose a *portal* parallel to the Y/Z plane.

The results of this subdivision were unusable. The local tangent is very sensitive to local disturbance of the skeleton, especially when the skeleton is 26-connected. This

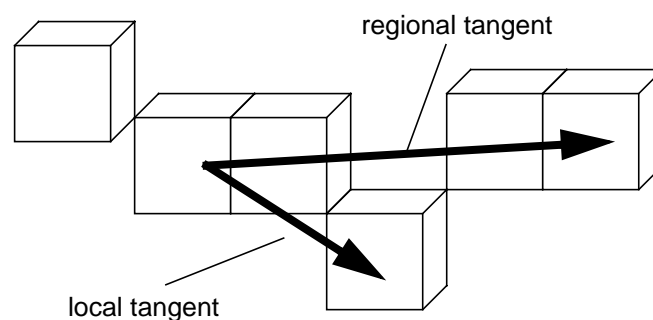


Fig. 3.5: A local correct, but regional incorrect tangent

resulted in *portals* which were parallel to the overall direction of this region of the skeleton and therefore, unusable. An extension to a regional tangent leads to the problem of establishing criteria to decide when a tangent becomes too global or too local.

Portal Size

This method takes into account the number of voxels which are part of the *portal*. The heuristic behind this method is that it is likely that a large *portal* is parallel to the regional direction of the skeleton and a small *portal* is rather perpendicular to the skeleton.

However, it turned out that this method generates long and narrow *portals* of small size but of an orientation parallel to the regional skeleton direction.

Gate ratio

The final method we present is dependent on the ratio of the length of the spanning sides of the *gates* (bounding boxes of the *portals*). Ideally, this ratio should be close to one to yield *gates* with a shape nearly square. It turned out that this method is a very robust scheme to compute the subdivision of the colon surface. In all examined datasets, the ratio to compute a “good” subdivision could be narrowed to the interval [0.7, 1.5].

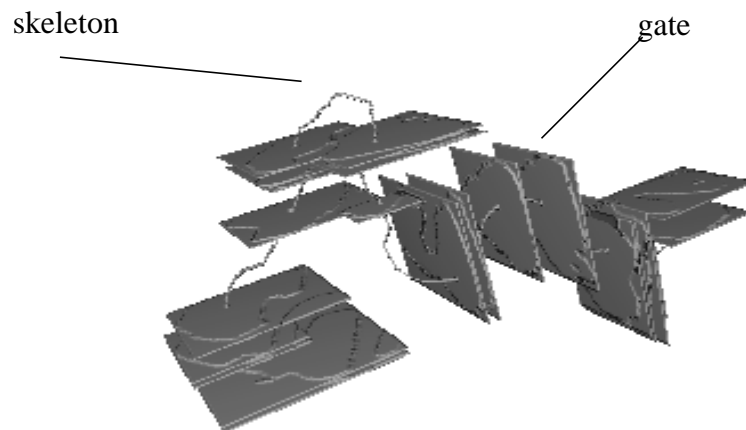
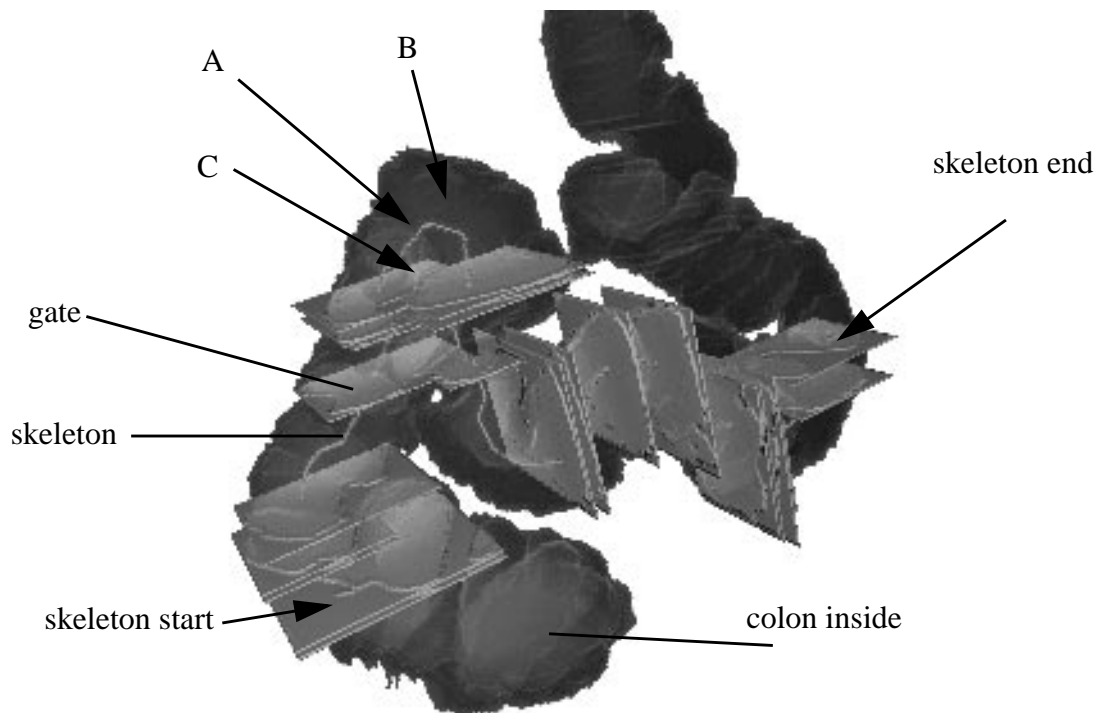


Fig. 3.6: A subdivision of dataset patient 9

Fig. 3.6 shows a typical subdivision; the *gate* and the skeleton of the colon are visualized. In *Fig. 3.7*, in addition to *gates* and skeleton, the inside voxels of the volume are rendered translucent. The absence of gates at the start and the end of the colon is due to the fact that the

skeleton does not start immediately at the beginning and terminates long before the actual end of the colon surface. This explains the high maximum values in *Tab. 2* of 188,823 triangles, although the subdivision in *Tab. 2* is not the same as the subdivision in *Fig. 3.6* or *Fig. 3.7*.

However, a usual subdivision of a dataset of this size (about 600K triangles) would consist of about 80 *segments*, while here we see about 20 *segments*.



**Fig. 3.7: Dataset patient9, with translucent inside voxels
(The gates at C are intersecting, not the portals themselves.)**

A general problem of the subdivisions is that we only use *gates* which are parallel to the three main planes of the cartesian coordinate system. This results in the inability to create a *gate* in a turn of the colon (see *Fig. 3.7, A*); we would get a non-effective subdivision which is not perpendicular to the colon direction. Another problem is the mandatory intersection rule; we cannot generate a *portal* at point B, because this *portal* would intersect the *portals* at C in *Fig. 3.7*.

```

subdivide(skeleton)
  start first skeleton voxel; mode = go;
  best_candidate = not_available;
  while not_end_of_skeleton do
    for planes i = xy, yz, zx plane do
      generate portal pi at voxel in plane i;
      if pi suffices_mandatory_criteria then
        if pi suffices_quality_criteria then
          store pi as candidate;
        else if pi is_better_than best_candidate then
          best_candidate = pi;
        fi;
        store pi as possible_candidate;
      fi;
    fi;
  od;
  if candidates_are_available then
    accept best_of_them;
    mode = go;
  else if possible_candidates_is_too_large then
    mode = accept_next;
  fi;
fi;
select mode:
go: go to next_voxel;
accept_next: if mode best_candidate is_available then
  go to best_candidate;
else stay_at_this_voxel;
fi;
tceles;
od;
end.

```

Algorithm 3.1: Subdivision along the skeleton

Algorithm 3.1 describe the subdivision scheme. Basically, we move along the skeleton and try to find a portal which suffices our mandatory and quality criteria. As soon as we know that we do not find a better portal, we accept an older one. If we do not have an older one, we accept the next portal we find.

3.2.3 The Visibility and Rendering Algorithm

Once the subdivision is generated, we can render the colon surface using our visibility and rendering algorithm. The essence of this algorithm is published in [HMHK96]. All *cells* of the colon are ordered in a sequential list with respect to their position along the skeleton of the colon.

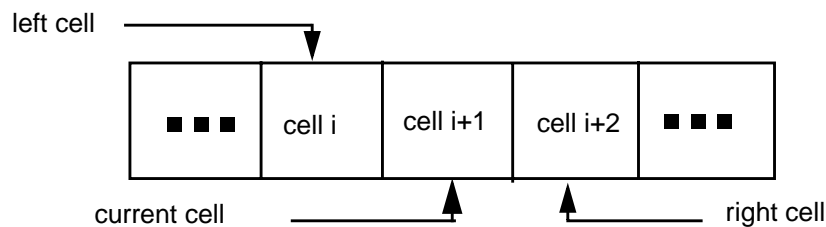


Fig. 3.8: Cell order

The algorithm in 3.2 describes the visibility check for the next *cell*, seen through its *gate* between the previous and the next *cell*. This algorithm is only applied on the *cells* which are preceding or succeeding the current *cell* - which contains the current camera position.

```

bool is_visible(next_cell, previous_gate)
  calculate position of gate of next_cell;
  if gate is_degenerated then return FALSE;
  if gate is_not_intersecting_with
    previous gate then return FALSE;
  if gate is_behind view point then return FALSE;
  if color_buffer has_no_empty_spots then return FALSE;
  else return TRUE;
end;

```

Algorithm 3.2: Cell visibility check

After calculating the projection of the *gates* of the next *cell*, we check if the *gate* is not degenerated, that is, if it is still a quadrilateral. If the *gate* is not intersecting the previous *gate*, it is not visible and all behind this *gate* is not visible. Therefore, we discard everything behind it. If the *gate* of the next *cell* is behind our view point, we discard this *cell* because it is not visible from this view point. If it is in front of our view point, we proceed with our check.

Finally, we check whether the color buffer still has some “empty spots”, that is, areas which are not filled by a rendered *cell*. If there are some “empty spots”, the following *cells* might be visible; otherwise, they are not visible.

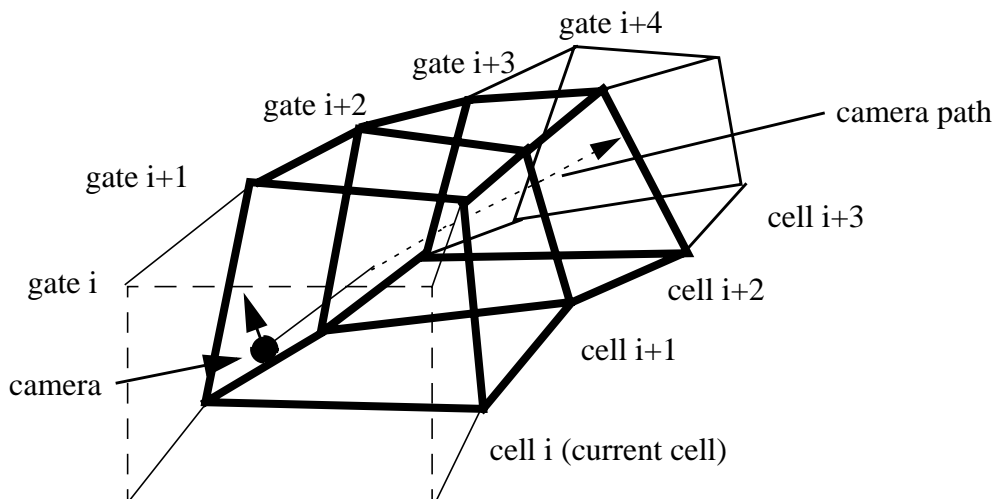


Fig. 3.9: Cell-visibility-check

In *Fig. 3.9*, the current camera position/view point is in *cell i*. Gate *i* (previous gate) and respectively *cell i-1* are behind our view point. Gate *i+1* is the gate of *cell i*; gate *i+1* is not degenerated and has a non-empty intersection with gate *i*. Furthermore, gate *i+1* lies in front of our camera. Suppose the color buffer in our example still has some spots which are not yet rendered. For these reasons, *cell i+1* is visible, and probably the same is true for *cell i+2*. The visibility of *cell i+3* is strongly dependent on the view point. From the current view point *i* our example, it is likely that *cell i+3* is not visible. However, gate *i+4* is not intersecting with gate *i+1*. Therefore, *cell i+4* is not visible.

Algorithm 3.3 describes the general rendering algorithm for the *cells* of the colon. We start adding the *cell* which contains the current camera position to a *cell* queue. All neighboring *cells* are added to the queue and are rendered, depending on their visibility and on their render-state; for further checking, the render-state must be inconclusive. The inconclusive mark is necessary to prevent loops, while the queue contains *cells* in both directions (right and left).

```
Forall frames do
  init queue and mark all cells as inconclusive;
  calculate current_cell of current camera
  position;
  add current_cell to queue and mark current_cell
  as visible;
  while queue is_not_empty do
    read first_cell from queue;
    get left_ and right_neighbors of first_cell;
    if left_cell is inconclusive and
      is_visible(left_cell, gate_of_current_cell)
    then add left_cell to queue;
      mark left_cell as visible;
    else mark left_cell as not_visible;
    fi;
    if right_cell is inconclusive and
      is_visible(right_cell, gate_of_current_cell)
    then add right_cell to queue;
      mark right_cell as visible;
    else mark right_cell as not_visible;
    fi;
    remove first_cell from queue;
  od;
od;
```

Algorithm 3.3: Colon check and rendering

In *Fig. 3.10* the algorithm starts with the initial rendering and marking of *cell i+1*, the *cell* with the current camera position/view point. Thereafter, we proceed with the cell-visibility-checks (algorithm 3.2) of the adjunctive *cells cell i+2* and *cell i*. Both are marked as visible or non-visible. Supposing the view direction is towards *cell i+2*, the check of the *cells* to the left of *cell i+1* (*cell i*, *cell i-1*) will stop after *cell i*. It only proceeds in direction of *cell i+2*, until the cell-visibility-check fails.

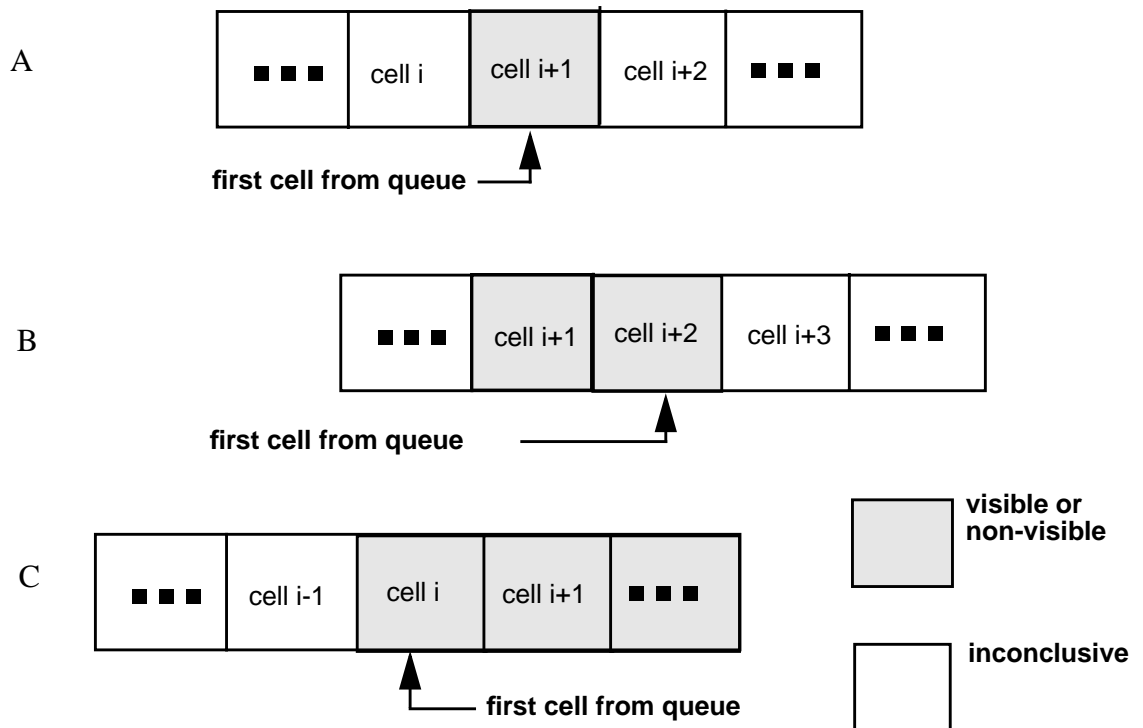


Fig. 3.10: Colon check: A initial step, B and C succeeding steps

3.2.4 Results

In this section, we present some rendering results of our Subdivision-, Visibility- and Rendering algorithm.

<i>Datasets</i>	<i>Total #Triangles/ #cells</i>	<i>Average #cells per frame</i>	<i>Average #Triangles per frame</i>	<i>Cellratio / Triangleratio</i>	<i>Average Frame rate</i>
Colon of the Visible Human	130,429 / 40	13	39,100	0.33 / 0.3	14.64
Patient 3	774,956 / 99	15	131,132	0.15 / 0.17	12.52
Patient 4a	836,774 / 89	4	45,948	0.04 / 0.05	17.12
Patient 4b	1,277,891 / 137	10	158,640	0.07 / 0.12	9.64

Table 3: Rendering results^a

- a. The data in this table are measured on a SGI Challenge with IR-graphics using one R10000 processor.

Table 3 contains the results of the measurements of four different datasets. Each of the datasets varies in size and granularity of the subdivision. Overall, we can observe that we achieved loss-free triangle reduction rates between 3.3 and 20. Directly associated with the reduction of triangles is the rendering speed and the frame rate. In any case, the dataset of the visible male is special; due to the different data acquisition, we obtained an already small number of triangles and a not very twisted colon. This led to a less successful performance of our visibility algorithm.

However, the right balance between *cell* size and number of *cells* is important; if the *cells* become too large, the render-overhead for non-visible parts of the *cell* deteriorates the rendering time. In cases of a large number of small *cells*, the number of costly visibility check will increase (patient 3, patient 4b). The reason for the high frame rate of the dataset patient 4a lies in the successful application of the visibility algorithm; a triangle reduction rate of 20 was obtained.

3.3 The Navigation Model

Most of the proposed navigation models for virtual endoscopy systems use a *planned- navigation* model. The flight path and the view direction for each frame is computed before the actual rendering. Any interaction is generally reduced to VCR-like functionality: Forward, Backward, Stop. Although this model is sufficient for an overview of the segmented data, it is not sufficient for a closer examination of the data because of the following reasons:

- Many data features are not visible from the pre-computed view point and view direction. Therefore these features will not be detected during the “flight” through the data.
- A **closer** examination of a “suspicious” area is not possible.

These limitations drastically reduce the usability of the system.

Complete freedom, however, in using the camera leads to severe orientation problems. The very twisted nature of the colon makes an orientation difficult. An inexperienced user can get lost easily.

In [HMHK96] an interactive navigation model is proposed, which adopts the paradigm of the *guided-navigation*. This paradigm gives the user the flexibility to interactively examine an area of the colon, but guarantees an orientation in the case of no user-interaction. The concept is based on the *submarine model*, inspired by the movie “Fantastic Voyage” [Flei66]. In this movie, a micronized submarine dives through the blood vessels of a human body. Like this submarine, our camera model is “diving” through a human colon.

Two major components control the *guided* movement of the camera: the attractive force - or potential hill - to the appendix¹ and the repulsive force of the colon wall. These forces are coded in a set of kinematic rules and in a *potential field* which is pre-computed during our third pre-processing step.

Fig. 3.11 gives an overview of the idea of the *potential field*. The appearance of the used *potential fields* can be seen in *Fig. 3.12* and *Fig. 3.13*; the attractive force is computed out of the *distance_from_exit* (*Fig. 3.12*), the repulsive force out of the *distance_from_boundary potential field* (*Fig. 3.13*).

Further discussion of the navigation model can be found in [HMBK97].

1. Like the blood stream in our submarine analogon.

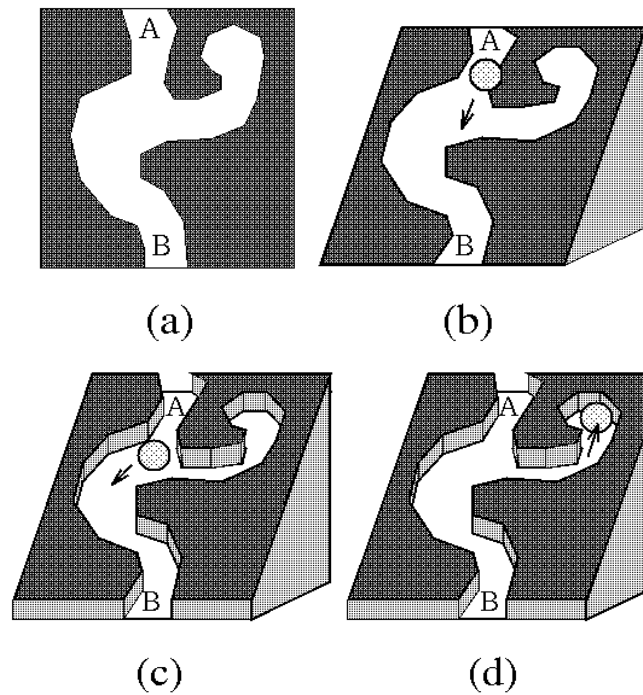


Fig. 3.11: From [HMHK96]: A: The topology of the colon. B: The submarine moves along the colon to the target, with respect to the potential hill. C: The potential field prevents the break through the colon wall. D: By applying a user specified force (direction), the user can move against the potential hill.



Fig. 3.12: The distance_from_exit potential field

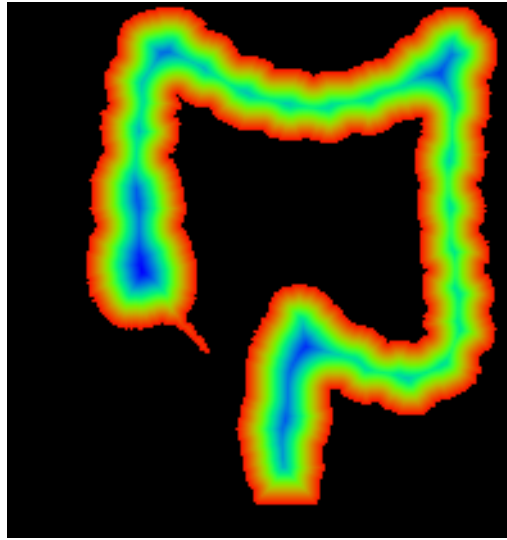


Fig. 3.13: The `distance_from_boundary` potential field

3.4 The User-Interface

One of the most critical issues in medical applications is a for physicians appropriate user-interface. Often, physicians are very sceptical about the usability of a new computer-based system. If this system does not sufficiently meet their needs or does not resemble already known technology, it may not be accepted. In our system, we developed a user-interface which - besides some advanced features - tries to simulate the “look and feel” of an optical colonoscopy. The VICON/i user-interface is constructed out of three main components, the main view (*Fig. 3.14*), the slice projection (*Fig. 3.15*) and the coronal projection (*Fig. 3.16*).

The main view contains the primary rendering area, which provides the ‘endoscopic view’ and the navigation control. In addition to the surface rendering, we have implemented a volume rendering algorithm, based on the PARC algorithm [ASK92]. We calculate the starting point of each ray from the corresponding z-value in the depth buffer, generated by the surface of the colon. The start point can be manipulated by a slider; we can choose a starting point

before or below the surface. This method, which we call peeling, simulates a virtual biopsy to examine the tissue below the surface.

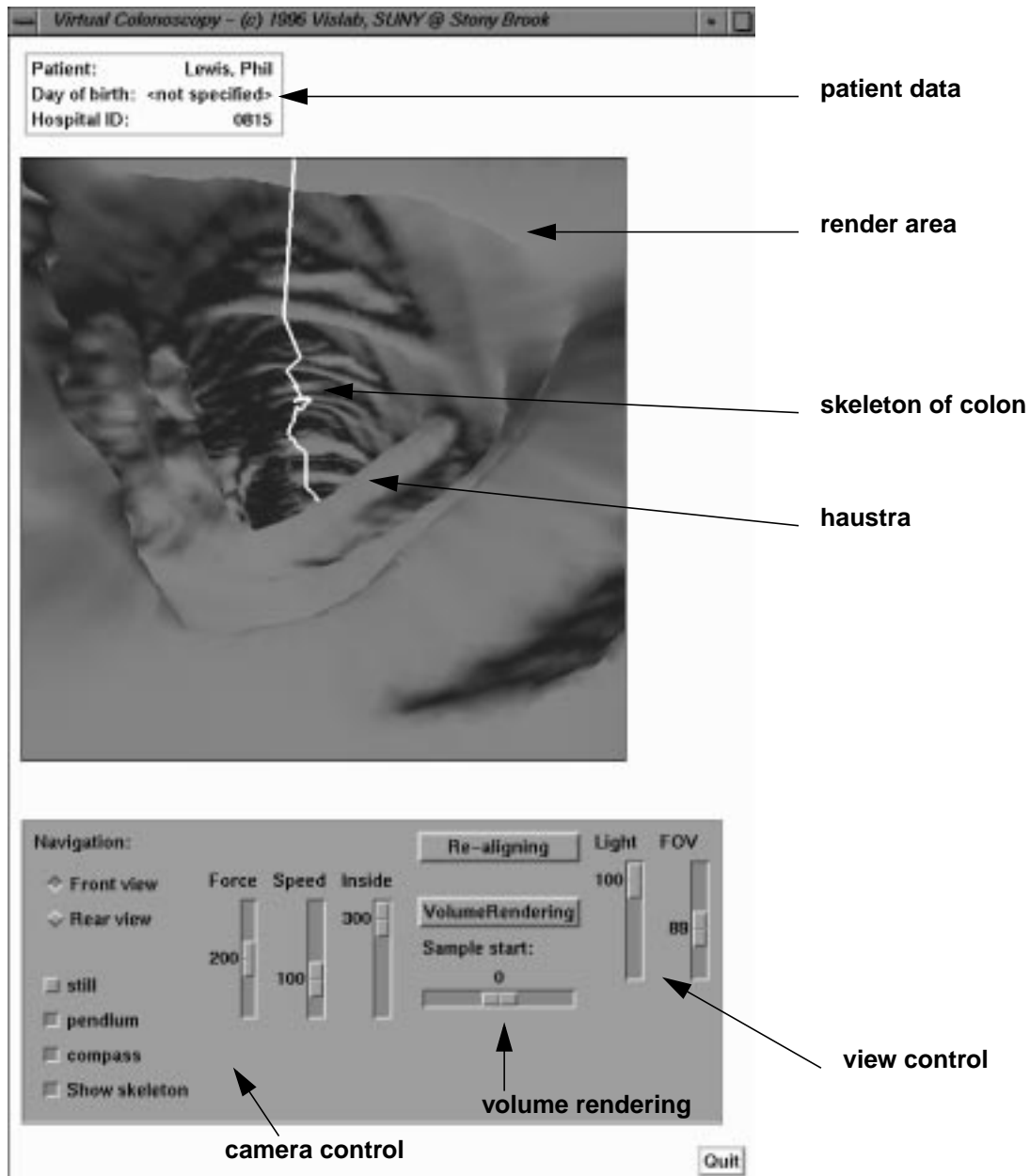


Fig. 3.14: VICON/i overview: The main view

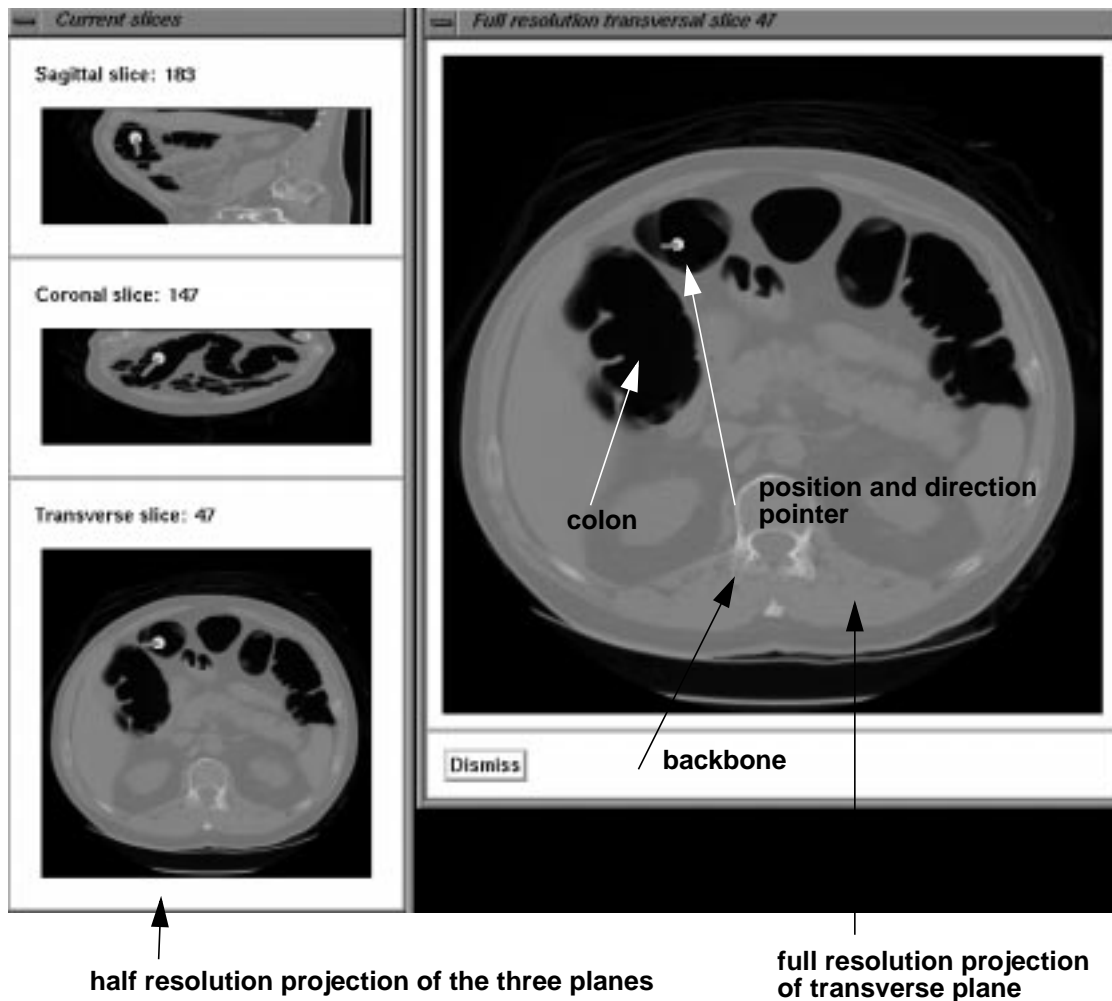


Fig. 3.15: VICON/i overview: The slice projections window

The second component of the user-interface, the slice projections, shows three orthogonal slices of the volume dataset - the sagittal, the coronal and the transverse slice, which are common in Radiology - at the current view point in half resolution. A full resolution slice can be shown, triggered by a mouse click on the corresponding half resolution slice. Additionally, the current view point is displayed in all slices.

Finally, the coronal projection provides an overview orientation of the colon. In contrast to traditional optical colonoscopy, which uses an uniform anatomy-textbook-like diagram of the colon, this projection is an accurate representation of shape and dimensions of the patient's

colon. Markers can be placed to mark a point of interest at the precise locations of polyps or other interesting structures.

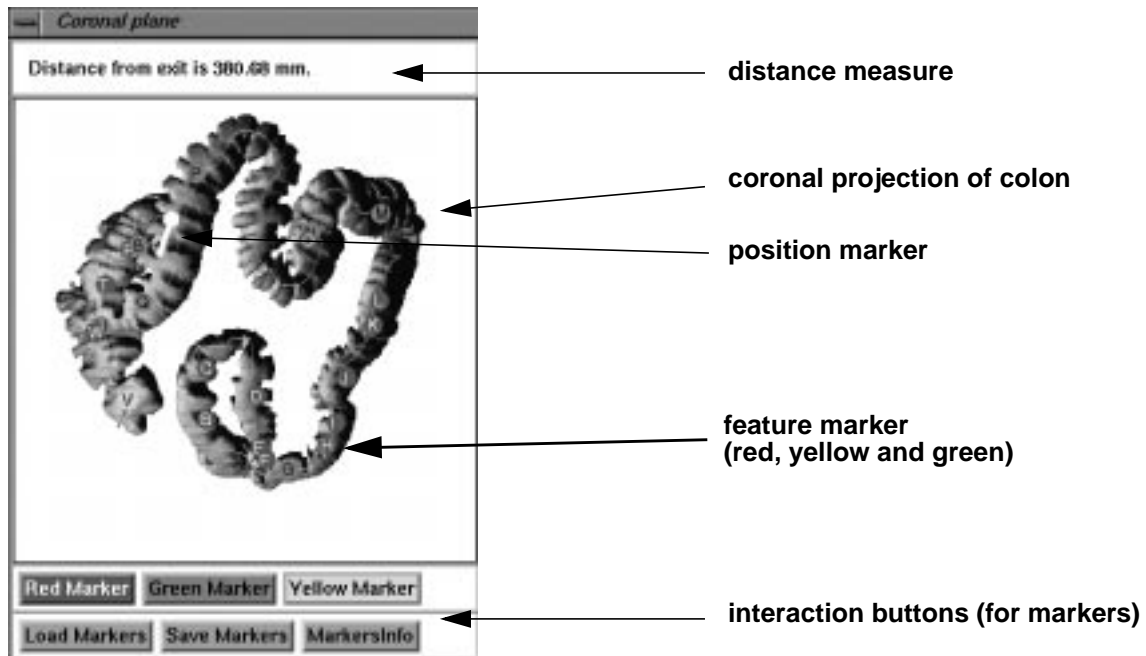


Fig. 3.16: VICON/i overview: the coronal projection

Similar markers of the optical colonoscopy (see *Fig. 4.1*) are not precise and can only be seen as rough approximations to the real location (*Fig. 3.17*). In contrast, the markers in *Fig. 3.16* are - within a small error tolerance - accurate and reflect the real locations of the markers in the same dataset as in *Fig. 3.17*.

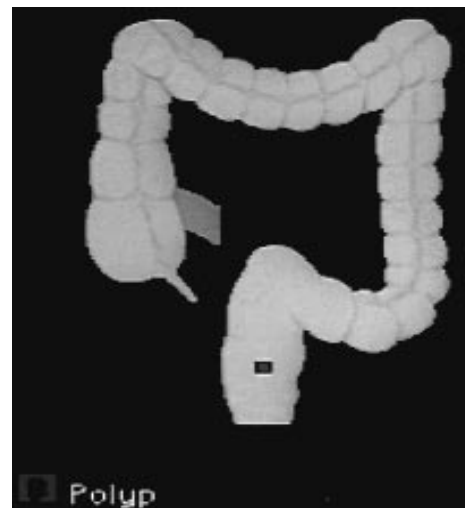


Fig. 3.17: A general diagram of a colon, generated by an optical colonoscopy

4. Two Methods for a Colonoscopy

In this chapter, we present two different methods for the exploration of the human colon. In first section we present in addition to section 2.2, some visual results of the optical colonoscopy of the same patient, who is subject of the virtual colonoscopy, presented in second section of this chapter.

4.1 A Optical Colonoscopy

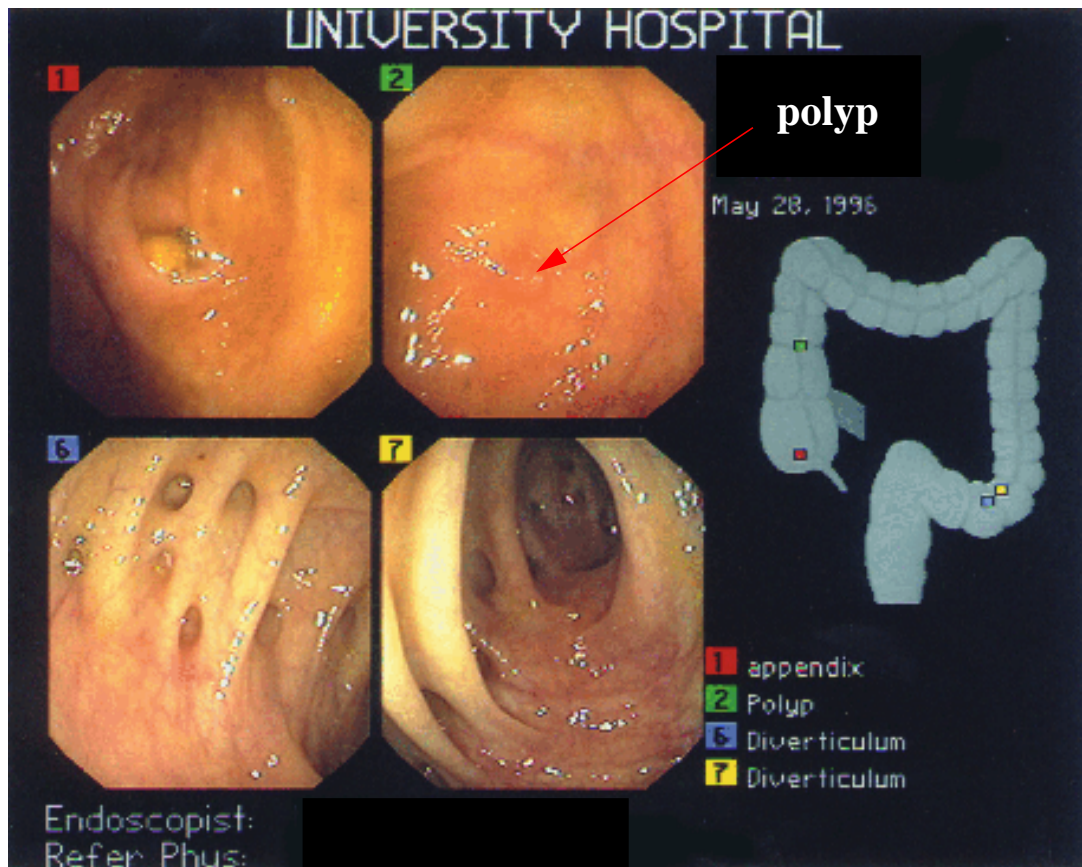


Fig. 4.1: Images from a optical colonoscopy

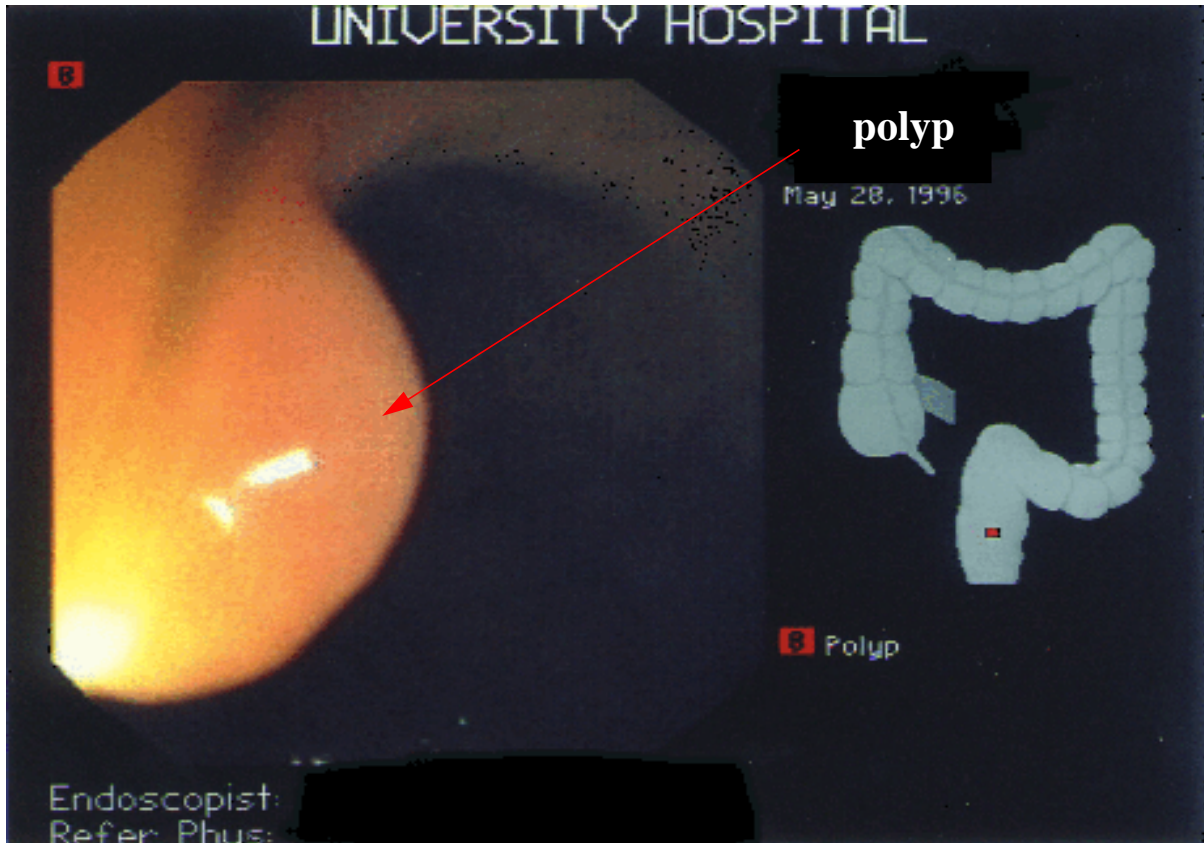


Fig. 4.2: A polyp, detected by an optical colonoscopy

The *Fig. 4.1* and *Fig. 4.2* show images from the optical colonoscopy. The first image shows four different views from the endoscope; the first view is at the end (respectively star) of the colon near the appendix. The second view shows a polyp in the ascending colon. The third and fourth view show shape anomalies called diverticulum, which are “holes” in the colon wall. A close-up to a polyp in an area close to the rectum - in the sigmoid colon - can be seen in *Fig. 4.2*.

4.2 A Virtual Colonoscopy

In this section, we present the results from the performed virtual colonoscopy. Note, this dataset is scanned from the very same patient, who underwent the optical colonoscopy of section 4.1.

Fig. 4.3 gives an overview of the examined dataset. We have set four marks, which represent areas of interests (AOIs). The views, associated with these marks and generated by the virtual colonoscopy, can be seen in *Fig. 4.4* and *Fig. 4.5*.

In contrast to the general colon shape of the optical colonoscopy (right side of *Fig. 4.1* and *Fig. 4.2*), the real shape of the colon of the patient is generated by the virtual colonoscopy. Additionally, the precise position of the suspected polyps with the correct distance from the reference point (start point or end point of the skeleton, usually associated with the rectum and the appendix) is represented in the marker information. This is a great aide for the physicians, who are performing the surgery to remove polyps. Finally, the current position and the view direction of the view point is shown.

The view at position marker B, can be seen in *Fig. 4.4*; this view represents a typical view inside of a human colon. The folds in the colon wall, haustras, are responsible for the wavy shape of this wall. In the same figure, on the right side, a shape abnormality can be seen. This abnormality could not be associated with a polyp of the optical colonoscopy. Therefore, it can be either an undetected polyp or stool.

Fig. 4.5 shows two different views of an interactive fly-through. In both views, we see a shape abnormality, which are suspected to be polyps. The positions are approximately the same, where the optical colonoscopy discovered polyps; the polyp in the left image, marker A, seems to be the same polyps as in *Fig. 4.2*. The right image, marker C, is at the approximated position of the polyp, shown in *Fig. 4.1*[2].

Views from a different dataset are shown in *Fig. 4.6*. We see a polyp in the dataset of the colon of the VisibleMale. On the left side, we see the surface representation of this view. On the right side, we can see a volume-rendered view overlaid with the surface representation. The shape of the polyp is visible in the purple color.

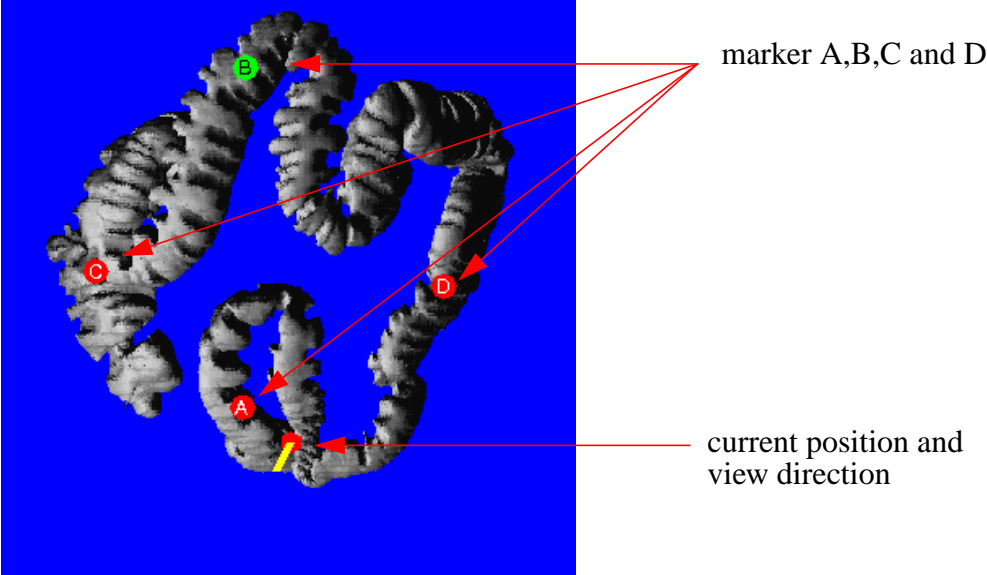


Fig. 4.3: Overview

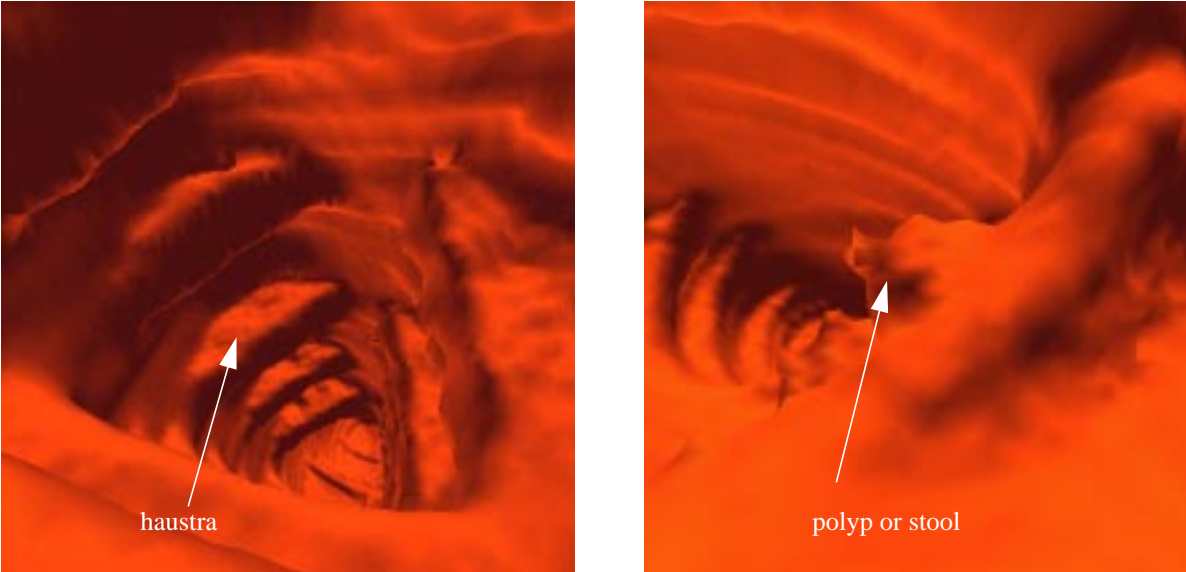


Fig. 4.4: Two views from the virtual colonoscopy; at marker C and D

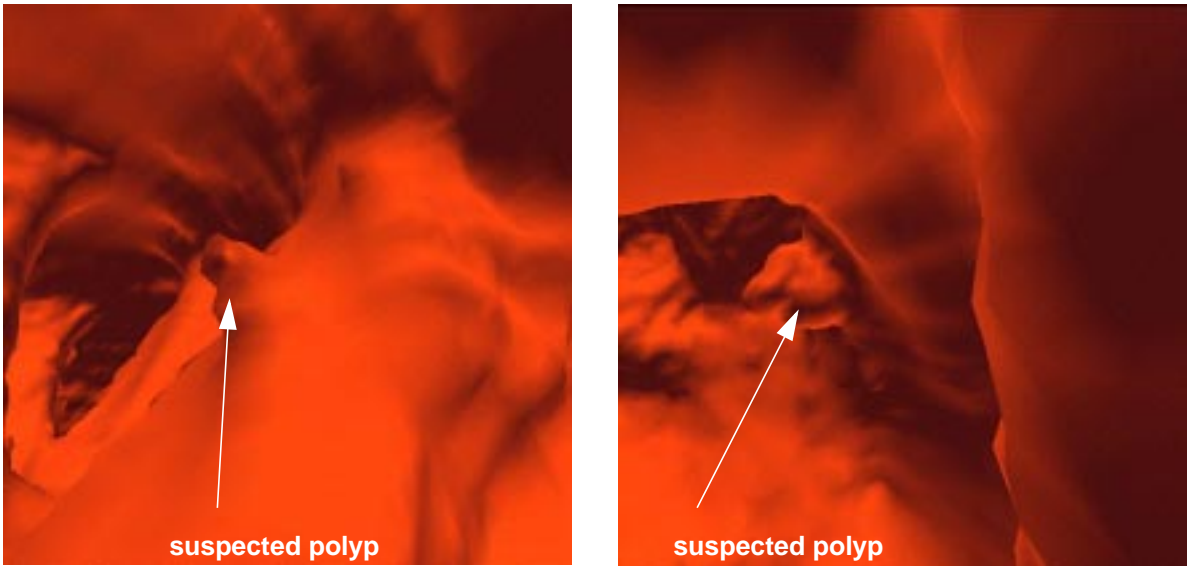


Fig. 4.5: Two views of polyps: A and C

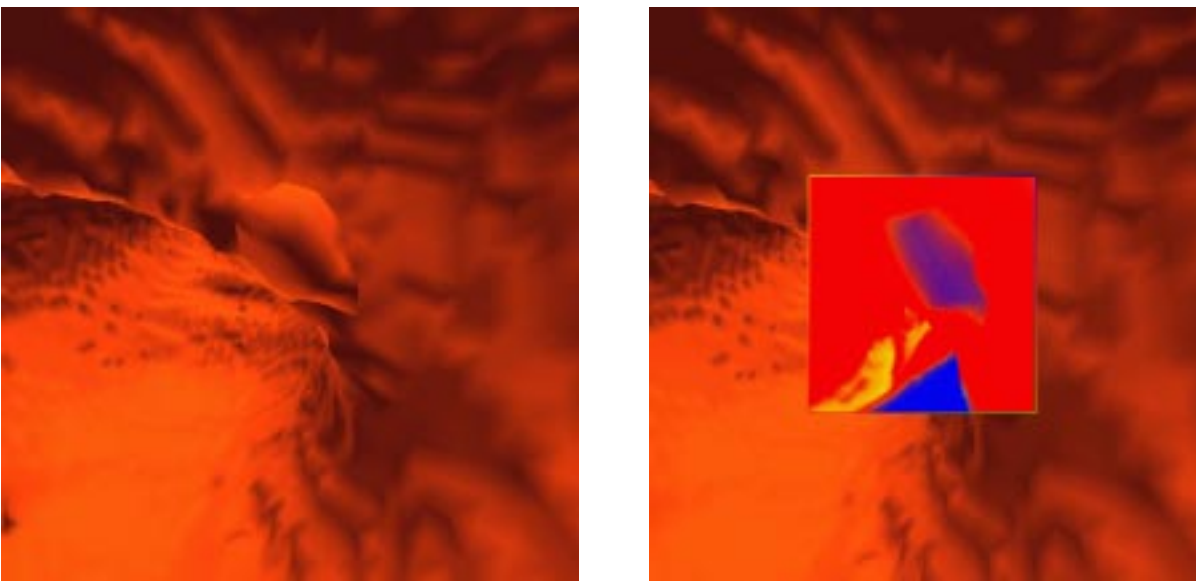


Fig. 4.6: Example of volume rendering

4.3 Discussion

In the preceding sections, the optical and the virtual colonoscopy have been described.

Shortly, a clinical evaluation will investigate the usability and the accuracy of the virtual colonoscopy system. However, early experience with our clinical partners of the Radiology are already available.

The handling of an optical endoscope and the orientation through the visual system of this endoscope is very difficult. Physicians are trained for a couple of years until they are able to operate successfully with this instrument. Our partners do not have this kind of training, which led to problems interpreting the optical colonoscopy, especially the current position, with the virtual colonoscopy. Nevertheless, they were able to use our system in less than half an hour. Although this is no proof of the usability of the system, it is promising.

A major challenge is still the segmentation of the data of the colon. The currently used binary segmentation is only sufficient for a completely clean colon. The appearance of stool inside of the colon, a very natural and common event, can not be distinguished from the actual surface. Unfortunately, the shape of not removed stool is close to the shape of a polyp. Therefore, a final statement whether this object is a polyp or stool is not possible. However, different methods to change the density values of the stool - with respect to the CT scan - seems to be possible. A closer investigation of this problem is on its way.

5. Conclusion and Future Work

5.1 Conclusion

In this thesis, we have presented an interactive virtual colonoscopy system, based on data extracted from a CT scan of the abdomen of a human body.

The interactivity of the system is based on a subdivision of the extracted surface of the colon dataset into cells. Based on this subdivision, a visibility check is applied to reduce the amount of triangle.

Several methods for this subdivision were investigated:

- a global versus a local approach
- three methods to decide whether a segment has an appropriate size
- three methods to generate an effective subdivision

It turned out that a combination of some of these methods generated feasible results.

1. We use a combination of a local approach and a limited correction ability to compensate for problems due to the unavailable global knowledge.
2. The heuristic using the number of surface or inside voxels of a segment to estimate the amount of triangles produced good results.
3. The ratio of the edges of the gates turned out to be a good criterion to decide whether the portals are perpendicular to the regional colon direction.

Depending on the size of the segments, respectively the cells, and of the general shape of the colon, the application of the visibility algorithm resulted in a high reduction rate of up to $1 / 20$. Only because of this reduction rate, was an interactive rendering of the colon possible.

An important issue of our system is the camera model, utilizing the guided-navigation paradigm. By default, the camera is controlled by the submarine model, which leads the camera along an center-path of the colon. At any time, the user can interactively manipulate the camera position and direction in order to focus the examination of the colon to a special part. This model combines the advantages of a planned-navigation and total-free navigation without their drawbacks. In practice, it shows a highly intuitive interaction, which quickly allowed our clinical partners to use this navigation model.

As segmentation method for the colon, a simple binary scheme is used. This is possible because of the strong contrast between the tissue of and behind the colon wall, and the air inside the colon. Although this scheme works reasonable well, it is not possible to differ stool from tissue; in some cases, a piece of stool can look like a polyp. Currently, different methods are investigated to change the density values of stool in order to differentiate it from tissue.

In addition to this problem, the density values of the polyps are very close to the density values of the usual tissue. Therefore, polyps can only be differentiated from this tissue by their shape.

5.2 Future work

Our future work can be divided into three groups:

- Solving existing problems
- Improving the rendering quality and extending functionality
- Extending the concept to other hollow organs/visceras

In this section, we will address several challenges coming from these groups.

- (1) As mentioned in the previous section, the segmentation of stool is a major issue for future work. The current assumption that the colon is completely cleaned of stool, is only an approximation of the actual situation; although the patient's preparation includes the cleansing of the colon of stool, it is usually not totally clean. To deal with this problem, the density values of the stool must be changed, in order to be able to segment it from the tissue.
- (2) A similar problem is the segmentation of polyps. Currently, this is not possible, because the polyp's density values in the CT dataset are not distinguishable from other tissue. Whether filter techniques like histogram equalization can solve this problem is yet unknown. However, using MRI data - instead of CT data - might solve this problem. An investigation of this approach is a major issue of the future work.
- (3) An important issue is an investigation of the clinical relevance of the virtual colonoscopy. Therefore, a clinical evaluation of this method is necessary, especially in comparison with the optical colonoscopy.
- (4) Currently, all the subdivision planes are parallel to one of the three main planes of the cartesian coordinate system. This leads to the problem that subdivision planes can fre-

quently not be generated in a twist of the colon; an orthogonal plane would be parallel to the colon direction rather than perpendicular (see plane A in *Fig. 5.1*). Additionally, the plane could not be created shortly after the twist because the corresponding portal would intersect the earlier generated portal (see plane B in *Fig. 5.1*). This problem can be solved, applying a non-perpendicular subdivision plane. However, this would involve a 3D scan conversion which is more expensive than the currently used simple orthogonal scan conversion.

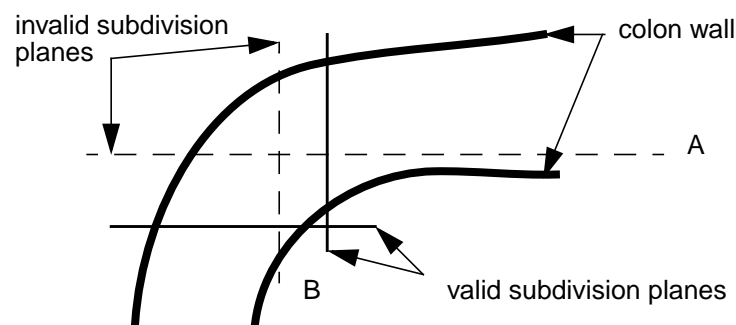


Fig. 5.1: Problems of the subdivision

- (5) An important part of the optical colonoscopy is the possibility of taking a tissue sample, using a small forceps which is introduced via the tube of the endoscope. Using this tissue sample, a histological examination, conducted by a pathologist, can be performed. A similar technique, a virtual biopsy would be useful in a virtual colonoscopy system. However, a closer examination of the virtual tissue sample is limited to the resolution of the CT scan. This resolution is coarser than the resolution of a microscope, used in the histological examination. Therefore, the virtual biopsy is not as usable as the real biopsy.
- (6) In the current system, a volume rendering component is implemented, using a peeling technique to examine voxels of the tissue below the surface. The development of meaningful transfer functions to visualize the relevant information is necessary. Furthermore, using the volume rendering as the basic rendering technique would improve the image quality. The multiprocessing ability of the available system - a SGI Challenge with 16 processors - would increase the frame rate, compared to the currently used single processor configuration.
- (7) The technology of a virtual colonoscopy system is not limited to examinations of the colon. In [LJK95], several other applications are presented. Especially, the explorations

of the stomach, the major blood vessels - i.e. the aorta -, the thorax, the abdomen and other hollow organs seem to be promising. However, different problems will be encountered while exploring other organs:

- The blood vessels are usually smaller than the colon and complex network of single tubular segments. This is a situation which requires a different subdivision than the current used subdivision.
- The stomach is not a tubular organ. Therefore, the effectiveness of the presented visibility algorithm is limited.
- The exploration of caverns of the body - like the thorax or the abdomen - makes a whole new segmentation and structure of the system necessary.

Appendices

A Class Structure of VICON/i

For the interactive part of the virtual colonoscopy system, VICON/i, several objects were implemented. For this system, we utilized the object-oriented software paradigm of communicating objects. Each of these communicating objects has its encapsulated data and its methods to manipulate this data. An overview of the interaction of objects can be found in *Fig. 5.2*.

The main interacting objects are:

- User-Interface - switches, sliders and buttons of the user-interface are implemented in this object. This object is communicating with the Render object and with the Camera Model to operate according to the parameters specified in the user-interface.
- Render - This object contains all the rendering routines for the fly-through. The following objects are children of the Render object, but not sub objects.
- Colon Projection - This object manages the Colon Projection window. The updates of the current position and direction of the view point are provided by the Render object. After a marker action redraws and new views are notified to the Render object.
- Slice Projection - This object displays the three orthogonal planes of the volume at the current view point. A pointer at the current view point with the current view direction is drawn.
- Volume Rendering - This object uses an implementation of a depth buffer based ray casting to generate a view of the volume.
- Camera Model - The position and the direction of the current view point, with respect to the navigation, is computed by this object. A new view, due to a marker action of the Colon Projection, can be passed via the Render object. Additionally, this object administers the potential fields, which are hidden from the other objects.

In addition to these objects, which are only used in VICON/i, are several other programs. These programs are responsible for the pre-processing stages, described in section 3.1.

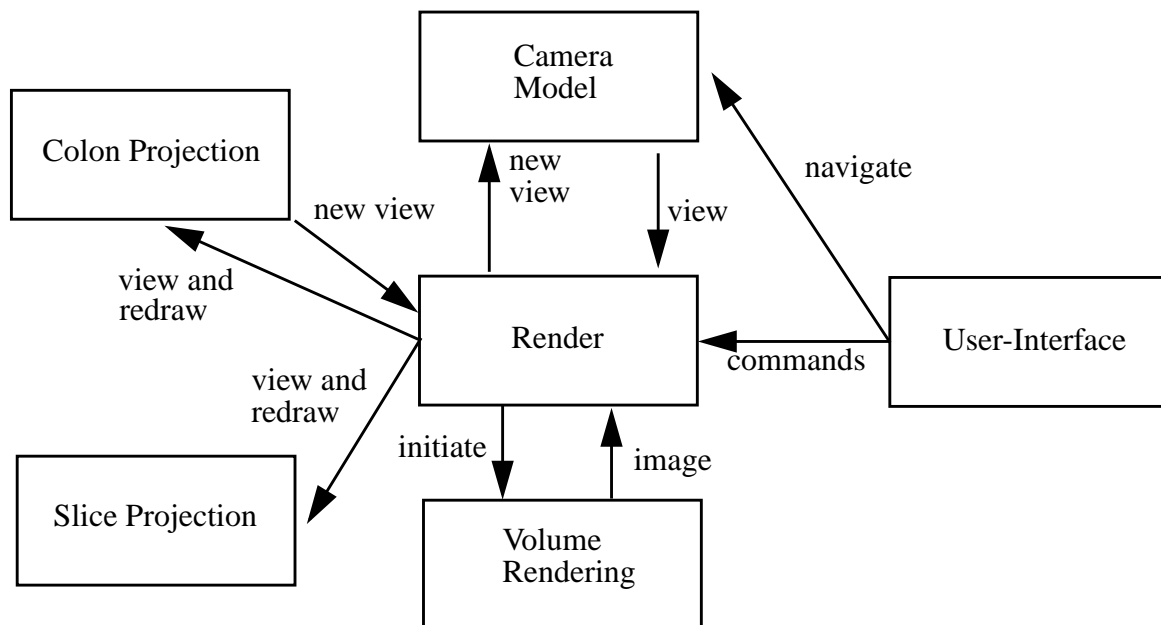


Fig. 5.2: Data flow of VICON/i

B File Structure of the Virtual Colonoscopy System

Throughout the system, several files are used to specify the boundary conditions of the fly-through. In this section of the appendix, we describe these files.

- slc - Besides the actual volume, this files contains information about the dimension of the dataset. The voxel number and the voxel sizes are provided to generate the view matrix. This file is used by the VolumeRendering and the Render object.
- mesh - The files in this directory specify the strips of the triangulation of the extracted colon surface. The strips can be processed by either GL or OpenGL. This file is only used by the Render object.
- ske - This file contains the skeleton voxels which are used by the several pre-processing

-
- steps (see section 3.1 for more information) and the rendering of the skeleton itself. It is used by the Colon Projection and Render objects.
- ins - This file contains the indices of the voxels which are classified as colon. It is used for several pre-processing steps, but not in VICON/i.
 - cpt - This files contains the distance or potential fields, which are only used by the Camera Model to compute the current view point.
 - info - This files contains information about the patient and is used by the User-Interface object.
 - sub - This file contains information about the subdivision, especially the position and dimension of the gates, which are necessary for the visibility algorithm in the Render object.
 - prm - This file specifies the parametrization of the algorithm to generate the subdivision.
 - markers - This files specifies the color and the position of the marker(s) of the last saved session. The Colon Projection object generates and uses this file.
 - map - This file contains all the indices of the voxels which are associated with the different segments of the subdivision. It is only used for the generation of the potential fields.
 - CORO, TRAN, SAGI - are the files with the three complete projections of the colon surface. The CORO file is used in the Colon Projection object to render the actual shape of the colon. The other files are currently not used.

The files ins, prm and map are only used in the several pre-processing stages of the system, VICON/seg, VICON/sub and VICON/p. Although this pre-processing stages are important steps of the presented system, only the subdivision step - VICON/sub - is described in section 3.2. Further information can be found in [HKWV95] and [HMBK97].

C References

- AKLS96 R. Avila, A. Kaufman, B. Lorensen, L. Sobierajski, R. Yagel. "Volume Visualization Algorithms and Applications". *Tutorial 1, IEEE Visualization '96*, 1996.
- ASK92 R. Avila, L. Sobierajski, A. Kaufman. "Towards a Comprehensive Volume Visualization System". *Proc. IEEE Visualization '92*, pp. 13-20, 1992.
- Bart95 D. Bartz. "Modelbased Manipulations of B-Spline Surfaces to simulate Deformations of the Facial Tissue". *Thesis*, Computer Science Department, University of Erlangen-Nürnberg, 1995.
- CBW95 L. Cohen, P. Basuk, J. Wayne. "Practical Flexible Sigmoidoscopy", IGAKU-SHOIN Medical Publishers Inc., pp. 1-9, 1995.
- DMS92 W. Dahmen, C. A. Micchelli, H.-P. Seidel, "Blossoming begets B-spline bases built better by B-patches", *Mathematics of Computation*, 1(1), pp. 97-115, 1992.
- Flei66 R. Fleischer (director). "Fantastic Voyage". 20th Century Fox, 1966
- FDFH92 J. D.Foley, A. van Dam, S. K. Feiner, J. F. Hughes. "Computer Graphics, Principles and Practice"^{2C}, Addison-Wesley, Reading, 1995.
- FLP89 H. Fuchs, M. Levoy, S.M. Pizer. "Visualization of 3D medical data". *Computer* 22, No. 8. pp. 46-51, 1989.
- HLVK96 L. Hong, Z. Liang, A. Viswambharan, A. Kaufman, M. Wax. "3D Reconstruction and Visualization of the Inner Surface of the Colon from SPiral CT Data". *Image Processing*, 1996.
- HKWV95 L. Hong, A. Kaufman, Y. Wei, A. Viswambharan, M. Wax, Z. Liang. "3D Virtual Colonoscopy". *Proc. 1995 Symposium on Biomedical Visualization*, pp. 26-32, 1995.

-
- HMBK97 L. Hong, S. Muraki, D. Bartz, A. Kaufman, T. He. "Interactive guided Examination of the Human Colon". Submitted to *Computer Graphics (Proc. SIGGRAPH'97)*.
- HMHK96 L. Hong, S. Muraki, T. He, A. Kaufman. "Physically-Based Interactive Navigation", *Technical Report TR 96.01.09*, Computer Science Department, SUNY at Stony Brook, 1996.
- HR85 W. H. Hollinshead, C. Rosse. "Textbook of Anatomy"⁴. Harper & Row, Philadelphia, 1985.
- HPRS94 K. H. Höhne, A. Pommert, M. Riemer, T. Schiemann, R. Schubert, U. Tiede, H. Krämer, C. Seebode, W. Lierse. "VOXEL-MAN/brain: A true 3D atlas of the human skull and brain", *Medizinische Informatik: Ein integrierender Teil arztunterstützender Technologien (Proc. GMDS'93)*, no. 77 in *Medizinische Informatik, Biometrie und Epidemiologie*, pp. 37-41, 1994.
- LC87 W. E. Lorensen, H. E. Cline. "Marching Cubes: a high resolution 3D surface construction algorithm", *Computer Graphics (Proc. SIGGRAPH'87)*, pp. 38-44, 1987.
- LJK95 W. Lorensen, F. Jolesz, R. Kikinis. "The Exploration of Cross-Sectional Data with a Virtual Endoscope". In R. Satava, K. Morgan (eds.), *Interactive Technology and New Medical Paradigm for Health Care*, IOS Press, pp. 221-230, 1995.
- KGCB96 R. M. Koch, M. H. Gross, F. R. Carls, D.F. Büren, G. Fanhauser, Y. I. H. Parish. "Simulating Facial Surgery Using Finite Element Models". *Computer Graphics (Proc. SIGGRAPH'96)*, pp. 421-428, 1996.
- KGPG96 E. Keeve, S. Girod, P. Pfeifle, B. Girod. "Anatomy-based Facial Tissue Modeling using Finite Element Method", *Proc. IEEE Visualization 1996*, pp. 21-28, 1996.
- Piep92 S. Pieper, "CAPS: Computer Aided Plastic Surgery", *Dissertation*, MIT, Cambridge, 1992.

-
- Stro93 B. Stroustrup, "The C++ programming language"², Addison-Wesley, Reading, 1993.
- VGBS94 D. Vining, D. Gelfand, R. Bechtold, E. Scharling, E. Grishaw, R. Shifrin. "Technical Feasibility of Colon Imaging with Helical CT and Virtual Reality". *Proc. Annual Meeting of the American Röntgen Ray Society*, pp. 104, 1994.
- VMW83 M. W. Vannier, J. L. Marsh, J. O. Warren, "Three dimensional computer graphics for craniofacial surgical planning and evaluation", *Computer Graphics (Proc. SIGGRAPH'83)*, pp. 263-273, 1983
- Wate87 K. Waters, "A muscle model for animating 3D-facial expression", *Computer Graphics (Proc. SIGGRAPH'87)*, pp. 17-24, 1987.
- WT90 K. Waters, D. Terzopoulos, "A physical model of facial tissue and muscle articulation", *Proc. of the First Conference on Visualization in Biomedical Computing*, pp. 77-82, 1990.